Spallation Reaction Physics

Antonín Krása

Neutron Sources for ADS

Declaration

This is a revised version of the manuscript for the lecture "Neutron Sources for ADS" for students of the Faculty of Nuclear Sciences and Physical Engineering at Czech Technical University in Prague. Please, be tolerant of mistakes.

Antonín Krása, Řež, May 2010

Contents

Chapter 1

Spallation reaction

1.1 Historical note

The observations of particle cascades in cosmic rays interactions have been done already in 1930's [1]. The thermal neutron flux density induced by cosmic-ray-protons is $\sim 10^{-4} - 10^{-3}$ neutrons cm^{-2} s^{-1} at the Earth's surface [2].

The first accelerator-driven spallation reactions have been discovered by B. B. Cunningham at Berkeley [3] in 1947. Theoretical description was given soon after by Serber [4]. W. H. Sullivan and G. T. Seaborg made up the term "spallation" in the same year [5].

Spallation reactions have been investigated for many years, but it has not been precisely described yet. They are being investigated with the increasing interest in the last two decades, as the spallation applications require more precise knowledge.

Spallation neutron sources are of interest for transmutation of long-lived actinides and fission products from nuclear waste [6], plutonium from nuclear weapons [46], or thorium (as an energy source) [43], material research and industry [9] or medicine for radiotherapy [10].

1.2 A course of spallation reaction

Spallation reaction is a process in which a light projectile (proton, neutron, or light nucleus) with the kinetic energy from several hundreds of MeV to several GeV interacts with a heavy nucleus (e.g., lead) and causes the emission of a large number of hadrons (mostly neutrons) or fragments. Spallation has two stages: intra-nuclear cascade and deexcitation, see **Fig. 1.1**.

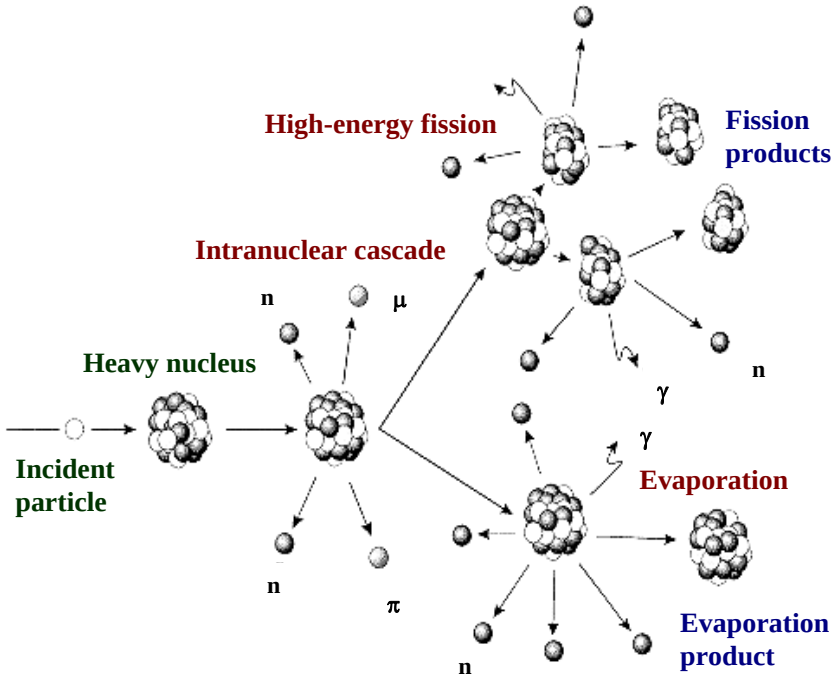

Figure 1.1: The scheme of a spallation reaction (according to [11]).

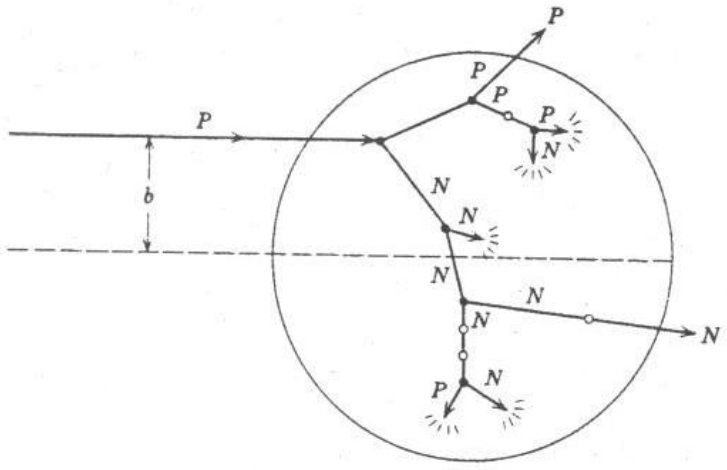

Figure 1.2: The scheme of an intra-nuclear cascade generated by a proton in a heavy nucleus with the impact parameter b. The solid circles represent the positions of collisions, the open circles represent the positions forbidden by the Pauli exclusion principle. The short arrows indicate "captured" nucleons, which contribute to the excitation of the nucleus (taken from [12]).

1.2.1 The intra-nuclear cascade (INC)

The **intra-nuclear cascade (INC)** is a fast direct stage ($\sim 10^{-22}$ s), see **Fig. 1.2**. As the reduced de Broglie wavelength of the ~ 1 GeV proton is ~ 0.1 fm, it interacts with individual nucleons in the target nucleus (instead of creating a compound nucleus). The projectile shares its kinetic energy with target nucleons by elastic collisions and a cascade of nucleon-nucleon collisions proceeds.

At low projectile energies (~ 100 MeV), all interactions occur just between nucleons and the process is called nucleon cascade [13]. Gradually, with growing incident particle energy, the threshold energies for particle production in nucleon-nucleon collisions are being exceeded. Initially, pions come up (at energies of about hundreds of MeV), at bigger energies ($\sim 2 - 10$ GeV) heavier hadrons are being produced. They can also participate in the intra-nuclear cascade and interact between each other, what is called hadron cascade [13]. Particles that obtain energy high enough to escape from the nucleus are being emitted mainly *in the direction of the incident particle*. The rest of the energy is equally distributed among nucleons in the nucleus which is left in a highly excited state.

The intra-nuclear cascade is not sharply separated from the equilibrium decay. In a pre-compound stage, the **pre-equilibrium emission** can happen[1]. In the course of this stage, fast particles or fragments may be emitted after each interaction between the incident or other cascade particle and a nucleon inside the nucleus. The energies of pre-equilibrium particles are greater than energies of particles emitted during the equilibrium decay.

1.2.2 Deexcitation

Finally, the equilibrium stage comes up ($\sim 10^{-16}$ s). Energy is equally distributed throughout the nucleus that is in a highly excited state with small angular momentum. The nucleus loses its energy by **evaporation** of neutrons or light charged fragments (e.g., d, t, α) with energies up to ≈ 40 MeV (which is the nuclear potential well depth [15]). The particles are emitted *isotropically* (in contrast to INC, see **Fig. 1.3**).

A competitive process to evaporation is **fission** (into two fragments similar in proton number). Fission products also undergo evaporation (depending on their excitation energy).

[1]For bigger beam energies and especially in heavy-ion collisions [14], multi-fragmentation (production of many fragments of relatively small charges) or breakup into individual particles are possible as well.

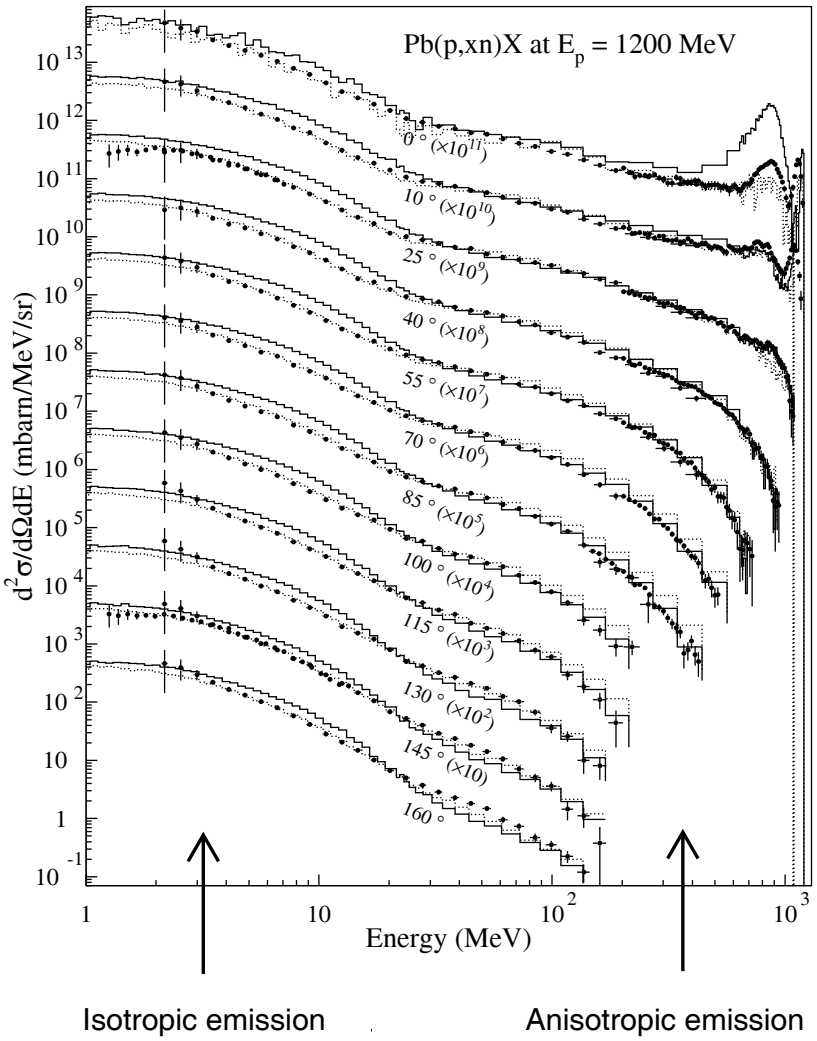

Figure 1.3: Neutron production double-differential cross-sections in reactions of 1.2 GeV protons on a thin Pb target (thickness of 2 cm). Each successive curve (from 160 °) is scaled by a factor of 10 with decreasing angle. Points are experimental values (measured at the SATURNE accelerator), histograms represent Bertini INC calculations (full lines) or INCL calculations (dotted lines). In order to obtain enough statistics, the emission angle in simulations was taken as ±2.5 °, while the experimental aperture was ±0.43 ° for $E_{\mathrm{n}} > 200$ MeV and between ±0.71 ° and ±0.81 ° for lower neutron energies (according to [16]).

When the nucleus does not have energy enough to emit neutrons (its excitation energy becomes smaller than the binding energy, typically about 8 MeV), it deexcites by γ-emission. After the termination of de-excitation by γ-transitions, the resulting nucleus is usually β-radioactive and decay until the stable state.

Two aspects of major importance in spallation reactions are residual nuclei (or spallation products) and emitted neutrons (or spallation neutrons).

1.3 Spallation products

The spallation products spread out in two regions of the chart of the nuclides, see **Fig. 1.4**. The upper right part corresponds to the heavy proton-rich residues produced from evaporation (spallation-evaporation products), the central part corresponds to the medium-mass residues produced from fission (spallation-fission products).

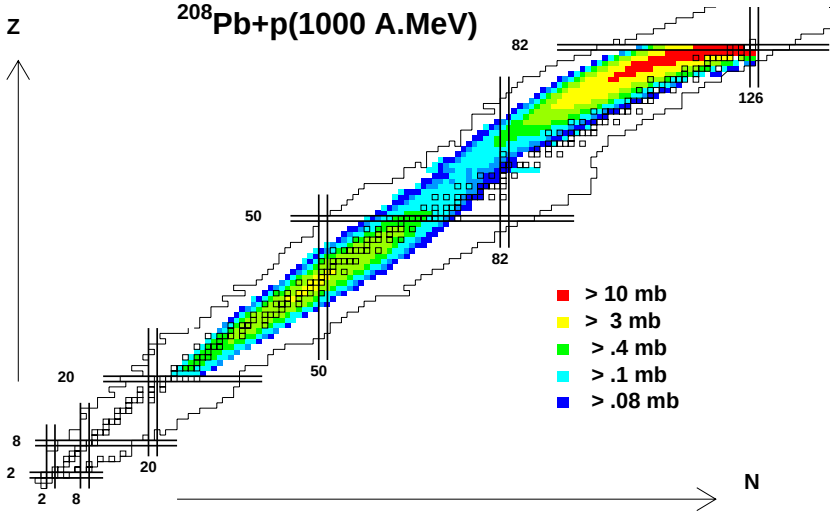

Figure 1.4: The cross-sections for residual nuclei production in the ^{208}Pb (1 AGeV) + p reaction. The distribution of the isotopes produced is shown on a chart of the nuclides, where black open squares represent stable nuclei, the magic proton and neutron numbers are indicated. Spallation-evaporation products and spallation-fission products are separated by a minimum of cross-sections at $Z = 58 \pm 3$. About 900 isotopes were identified, the total reaction cross-section amounts to $\sigma_{\mathrm{tot}} = (1.87 \pm 0.23)$ b (according to [19, 21]).

The spallation products can be measured using two methods: direct [17, 18] or inverse kinematics [19].

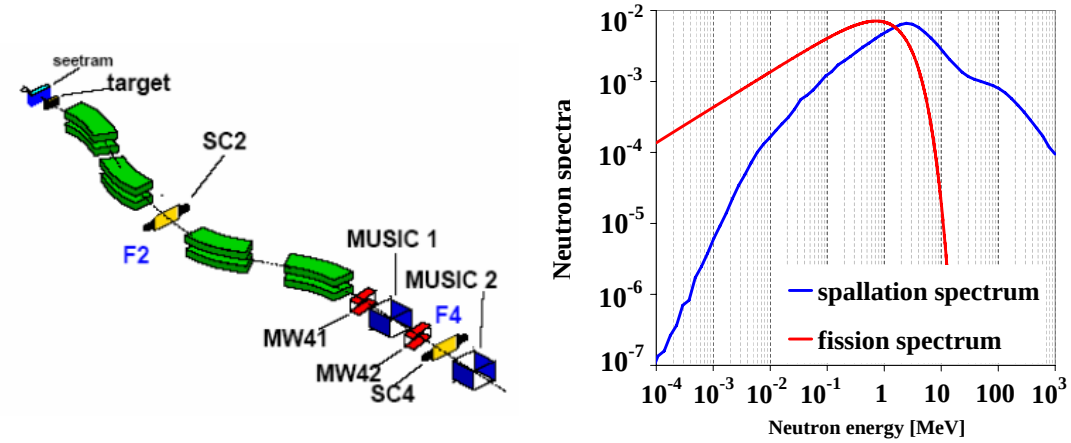

Figure 1.5: Left: Schematic view of FRS in GSI (Gesselschaft für Schwerionenforschung) Darmstadt, Germany (taken from [22]).
Right: Spallation neutron spectrum (MCNPX simulation of neutron production in p+Pb at 1 GeV; an arbitrary normalization) and fission spectrum ($\chi = \sqrt{\frac{2}{\pi e}}\exp(-E)\sinh(\sqrt{2E})$; according to [11]).

1.3.1 Direct kinematics

In direct kinematics, a relativistic light projectile hits a heavy target. The spallation products, which stop in the target, can be detected using γ-spectroscopy and mass spectrometry.

This method has the possibility to measure the yields of the meta-stable states of residual nuclei, it can use radioactive targets, and it consumes less beam time. On the other hand, it is impossible to measure the yields of very long-lived, stable, and very short-lived nuclei, and the off-line yields measurements are more time consuming.

1.3.2 Inverse kinematics

In the case of inverse kinematics, a relativistic heavy nucleus hit a light target. The spallation products leave the target in forward direction and can be identified immediately in flight using the appropriate technique.

The example can be the magnetic spectrometer FRS (FRagment Separator) [20] consisting of four dipole magnets (plus sets of quadrupoles and sextupoles) and the following detector equipment (**Fig. 1.5** left): a beam monitor (seetram), an energy degrader (placed at F2) causing energy losses of the transiting nuclides depending on their charge, two position-sensitive plastic scintillator detectors (SC2, SC4) measuring horizontal position of the

transiting nuclides and time of flight (TOF) over the flight path of 36 m from each other, multiple-sampling ionisation chambers (MUSIC), and multi-wire proportional counters (MW).

1.4 Spallation neutrons

The neutrons produced in spallation reactions can be characterized by their energy and spatial distributions and multiplicity.

1.4.1 Neutron spectrum

Spallation neutron spectrum extend from the beam energy down to tenths of keV with the maximum around 2 MeV and differs so from fission neutron spectrum that reaches from thermal energies up to app. 10 MeV with the maximum around 1 MeV, see **Fig. 1.5** right.

Spallation neutron spectrum[2] can be decomposed into four components, each of which represents a single physics process leading to neutron production [23] (see **Fig. 1.6**):

$$\frac{\mathrm{d}^2\sigma}{\mathrm{d}\Omega \mathrm{d}E} = A_1 \exp\Big(-\frac{E}{E_1}\Big) + \sum_{i=2}^{3} A_i \exp\Big(-\frac{E}{E_i}\Big) + \\ + A_{\mathrm{el}} \exp\Big[-\Big(\frac{E-E_{\mathrm{el}}}{W_{\mathrm{el}}}\Big)^2\Big] + A_{\mathrm{inel}} \exp\Big[-\Big(\frac{E-E_{\mathrm{inel}}}{W_{\mathrm{inel}}}\Big)^2\Big], \quad (1.1)$$

where the evaporation component, cascade component, quasi-elastic component (correspond to peripheral collisions when neutron is ejected after one elastic collision), and quasi-inelastic component (the same as the latter, but leaving the partner nucleon excited to the Δ-resonance) stand in this sequence. Of course, the quasi-elastic and quasi-inelastic components are inconspicuous at backward angles, see the lower part of **Fig. 1.6**.

The quantity E_{el} (E_{inel}) is the average energy of the neutrons that are ejected after a single (in)elastic collision induced by the incident proton. The quantity $E_{\mathrm{inel}}(0^{\mathrm{o}})$ differs from the incident energy because of the Fermi motion of the struck nucleon (and the influence of the Pauli blocking, which may inhibit the collision). The quantity W_{el} reflects the "width" of this

[2]The double differential cross-section $\frac{\mathrm{d}^2\sigma}{\mathrm{d}\Omega \mathrm{d}E}$ is defined as the number of neutrons that are scattered into the solid angle interval (Ω, $\Omega + d\Omega$) and into the energy interval (E, $E + dE$). It is normalized to $d\Omega$, dE.

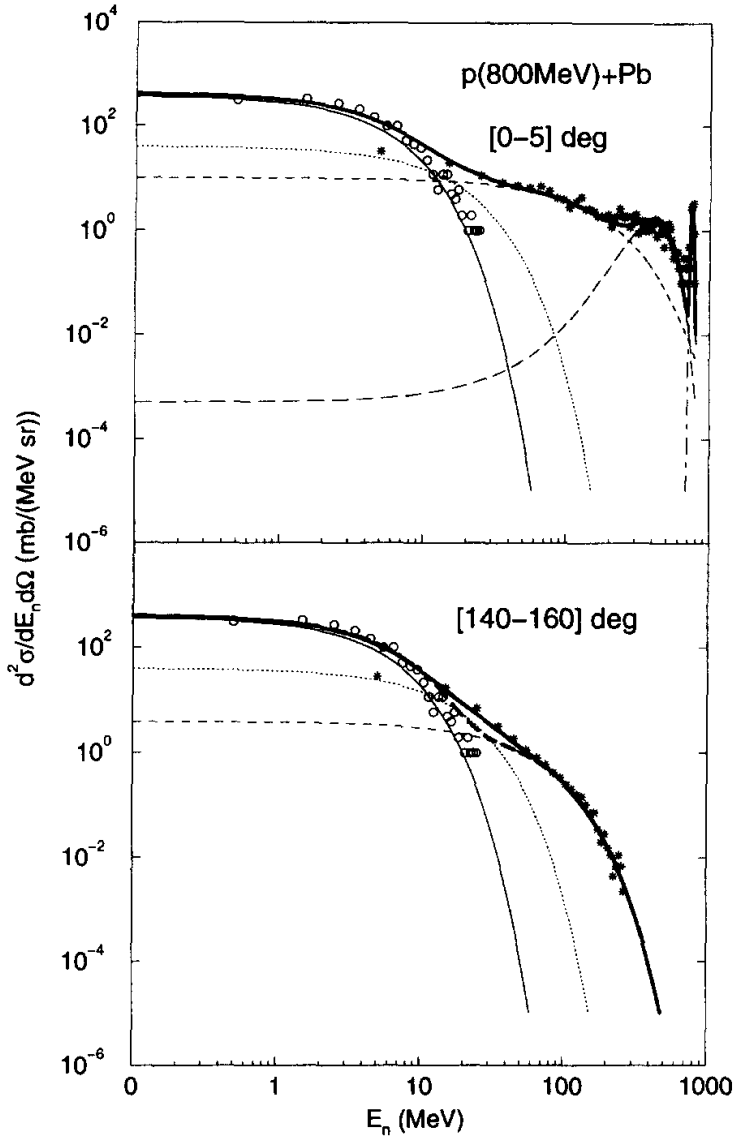

Figure 1.6: Neutron production double-differential cross-section in reactions of 0.8 GeV protons on a thin Pb-target. The upper part is averaged over angles $0-5^o$, lower part is averaged over angles $140-160^o$. The symbols give the results of INCL+Dresner simulation: stars stand for cascade component, open circles for evaporation. The thick curve represents the fit of the results by formula (1.1), thin curves represent various components: full curve – evaporation, dotted and small-dashed curve – cascade, long-dashed curve – quasi-inelastic, and dot-and-dashed curve – quasi-elastic components. The thick dashed curve (in the lower part) represents the fit when only one exponential in the cascade component of formula (1.1) is leaved in (taken from [23]).

Fermi motion (with the influence of the Pauli blocking). The width W_{inel} is dominated by the width of the produced Δ-particle, which is much larger than the width of the Fermi sea. The physics meaning of the width parameters $E_{1,2,3}$ is not obvious. The parameters E_i and amplitudes A_i depend on the target mass (in the case of U-target, it is necessary to take into account also extra neutrons emitted by the excited fission products).

The fact that the cascade component cannot be fitted by one exponential function (which is indicated in the lower part of **Fig. 1.6**) reflects the process complexity. On the other hand, it can be perceived as a surprise that the multiple collision part of the cascade could be simply described by two exponentials.

The experimental results of energy and spatial distributions of the neutrons produced in spallation reactions show the same trends as simulatons, see **Fig. 1.3**. The quasi-elastic and quasi-inelastic contributions disappear above 25 °. Neutrons with energies from 3 to 400 MeV have been detected by the time-of-flight technique (the time difference between the incident proton, tagged by a plastic scintillator, and a signal from a neutron-sensitive liquid scintillator) [24]. Neutrons with energies bigger than 200 MeV (where the TOF resolution is poor) have been detected using (n,p)-scattering on a liquid hydrogen converter and reconstruction of the proton trajectory in a magnetic spectrometer [25]. The angular distribution of neutrons have been measured by an additional collimation system.

1.4.2 Neutron multiplicity

The number of neutrons produced per one beam particle is called **multiplicity**. Neutron multiplicity as a function of the beam energy and target material shows roughly linear dependence on the target mass number (in the range $12 < A < 238$) and slow increase with incident proton energy (in the range $0.2 < E_{\mathrm{p}} < 2$ GeV). The semi-empirical formula ([23]):

$$M_{\mathrm{n}}(E_{\mathrm{p}}[\mathrm{GeV}], A) = (0.0803 + 0.0336 \ln(E_{\mathrm{p}}))A \tag{1.2}$$

gives better than 10% accuracy for $A > 40$, see **Fig. 1.7**.

The share of cascade and evaporation neutron components depends on the beam energy. Broadly speaking, the evaporation contribution is more important than the cascade one by a factor of 2 for $E_{\mathrm{p}} > 1$ GeV; its importance is reduced at lower energies [23]. The cascade component is roughly a linear function of target mass number and only weakly depend on proton energy, see upper part of **Fig. 1.8**. The evaporation component is also almost a linear function of target mass number but it depends much more on proton

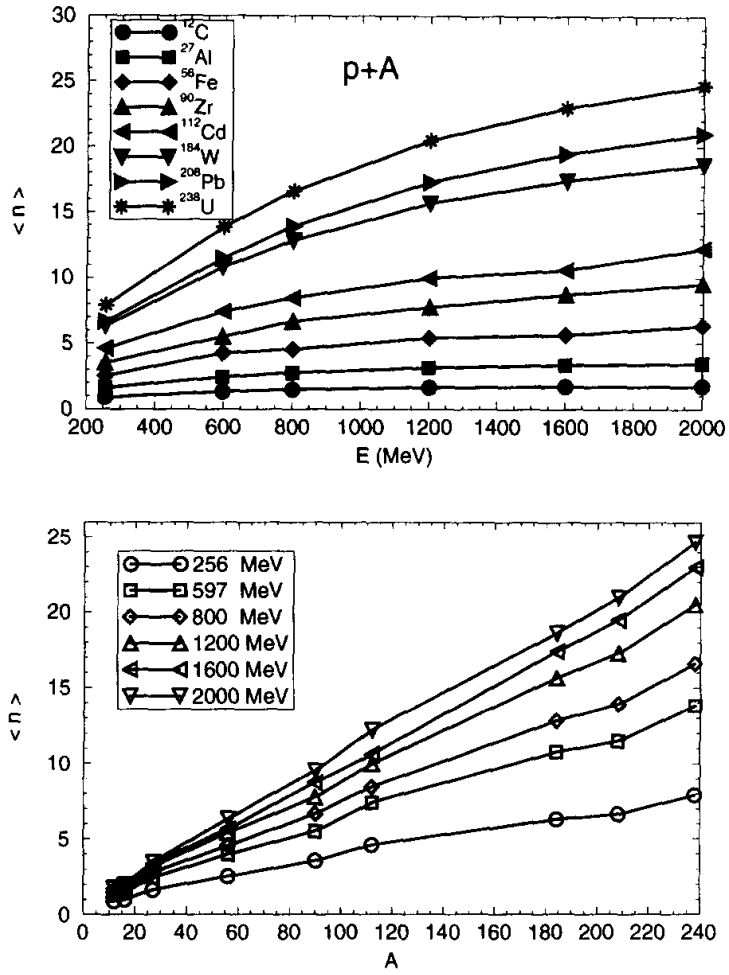

Figure 1.7: Neutron multiplicity per incident proton as a function of beam energy (upper part) and (thin) target material (lower part). Results of INCL+Dresner simulation (taken from [23]).

energy, see lower part of **Fig. 1.8**.

In the case of INC, the most important is the number of collisions made by the incident particle. This parameter does not change strongly with incident energy, because the nucleon-nucleon cross-section does not change much in the considered energy region.

In the case of evaporation, the number of emitted neutrons depends mainly on the excitation energy left in the target nucleus at the end of the cascade stage. This excitation energy increases (slightly less than linearly) with the proton beam energy (see **Fig. 1.9**).

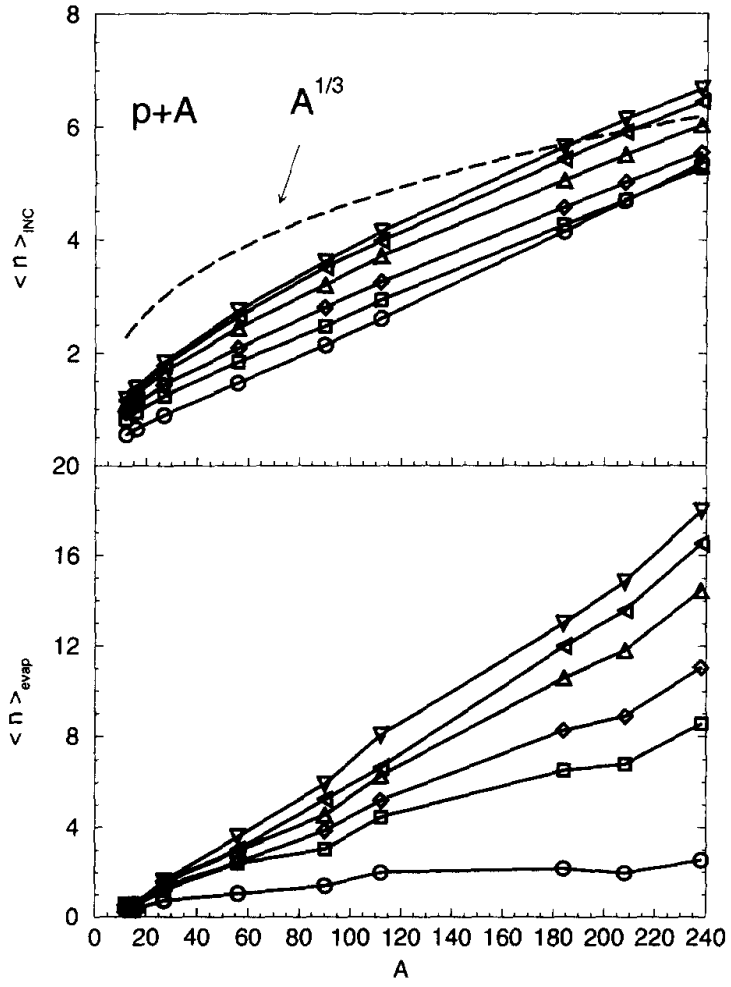

Figure 1.8: Neutron multiplicity as a function of (thin) target material. Split into cascade (upper part) and evaporation components (lower part). Open symbols refer to the values of the incident energy, with the same convention as in the previous figure. Results of INCL+Dresner simulation (taken from [23]).

1.5 Spallation reactions on thick targets

In the case of a thick target, high-energy particles escaping from the nucleus in the course of INC can induce further spallation reactions and generate **inter-nuclear cascade**. It relates mainly to neutrons because they do not lose their energy by ionization losses. Thus, among all emitted particles, they penetrate deepest into the target material. For some target materials, low-energy spallation neutrons (i.e., low-energy cascade plus evaporation neutrons) can enlarge neutron production by **(n,*x*n)-reactions**.

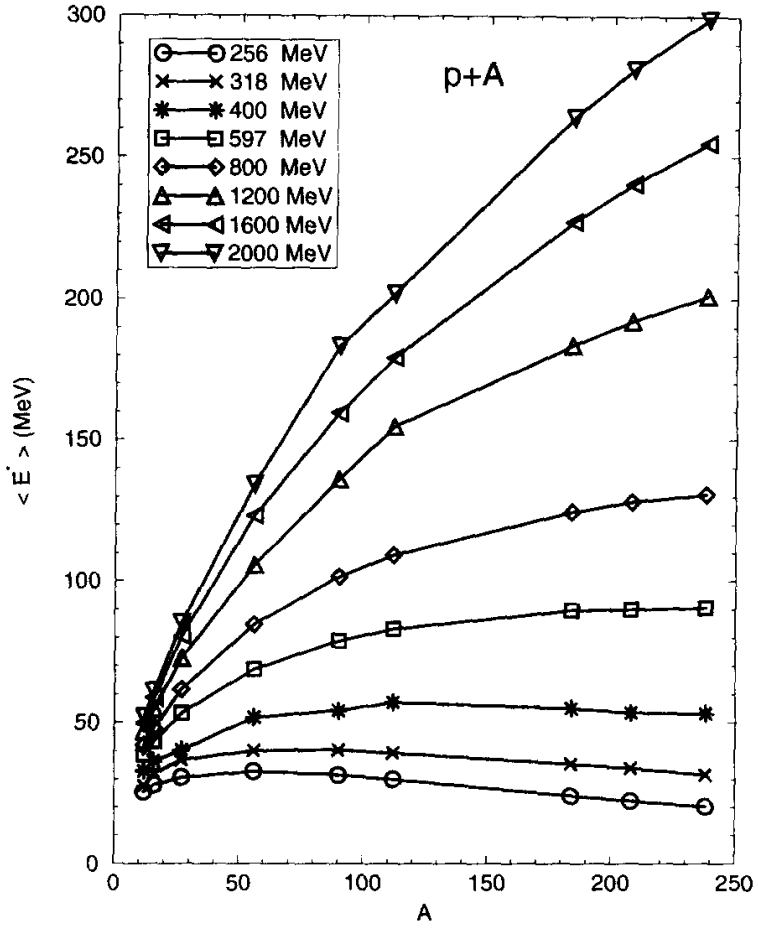

Figure 1.9: The excitation energy left in the target nucleus after INC in proton-induced reactions at several incident energies as a function of target mass (taken from [23]).

Globally, the incident proton induces the production of a large amount of neutrons (**Fig. 1.14**) with wide energy spectra (**Fig. 3.2**). The neutron multiplicity for thick targets depends on the projectile-target combination.

Thick target neutron multiplicity can be calculated as

$$M_{\mathrm{n}}(x_{\max}) = \int_0^{x_{\max}} M_{\mathrm{n}}(E_p(x)) N_p(x) n_j \mathrm{d}x, \tag{1.3}$$

where $M_{\mathrm{n}}(E_p(x))$ is the thin target neutron multiplicity expressed by the formula (1.2). The beam intensity is

$$N_p(x) = N_0 \exp(-\frac{x}{\lambda}), \tag{1.4}$$

where $\lambda = \frac{1}{n_j \sigma}$ is the mean free path, n_j is the number of target nuclei per unit volume, σ is the reaction cross-section.

1.5.1 Projectile type and energy

Besides protons, other light nuclei or hadrons beams have been investigated. The deuteron-induced spallation reactions on thick targets were explored theoretically [26] using the LAHET+MCNP codes. Neutron production in deuteron-induced reactions is bigger than in proton-induced ones by a factor of 1.3-2.5 for light targets and small beam energies, but it is more or less the same (within 10%) for heavy targets and bigger beam energies (**Fig. 1.10**), which are considered for ADS purposes.

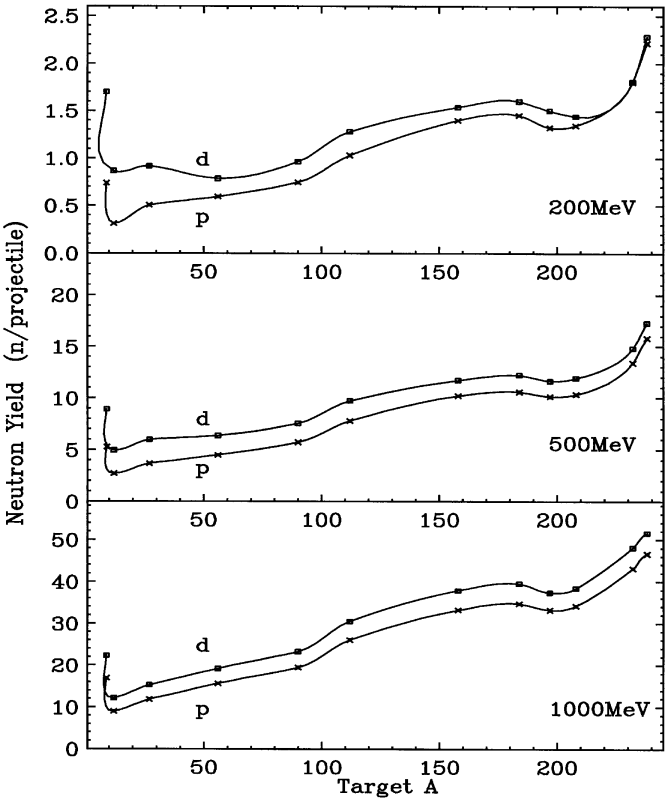

Figure 1.10: Neutron multiplicity as a function of target material for 200, 500, 1000 MeV protons and deuterons. A thick target (cylinder with equal length and diameter given by two ranges for protons depending on incident energy) was used for LAHET+MCNP simulation (taken from [26]).

A set of experiments with 3.65 *A*GeV light nuclei beams was carried out

at JINR Dubna [27] in 1980's with conclusion that the number of neutrons produced per one incident proton as well as the power consumption for neutron generation are slightly preferable for light nuclei (^{2}H, ^{4}He) to protons, while neutron production for heavier projectiles (^{12}C) decrease because of higher Coulomb potential. But this is valid for beam energies $\gtrsim$ 3 AGeV only; the ionization losses of ions increase significantly for beam energies around 1 GeV, which is expected optimal energy region for future ADS.

Recent experiments carried out at CERN [28] show that the proton-, antiproton-, charged pion-, positive kaon-, and deuteron-induced reactions in the energy range of 1-6 GeV result in very similar neutron multiplicities, see **Fig. 1.11**. So, the neutron multiplicity is relatively independent of the incident hadron species.

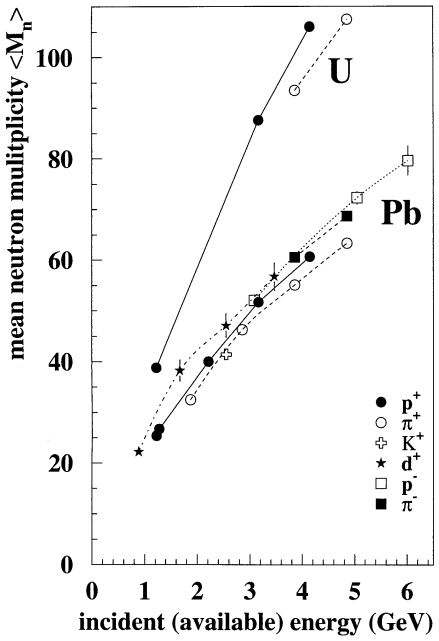

Figure 1.11: Neutron multiplicity as a function of beam energy (for different beam particles) on thick lead (length of 35 cm, diamater of 15 cm) and uranium (length of 40 cm, diamater of 8 cm) targets. The curves connect the data points (taken from [28]).

Neutron multiplicities can be investigated using a liquid-scintillator detector with large angular acceptance, e.g., the 4π BNB (Berlin Neutron Ball) detector [32] and the ORION detector [33] consist of a spherical shell filled with liquid scintillator (which slow the produced neutrons by scattering with H and C nuclei) loaded with Gd that capture the moderated neutrons. The

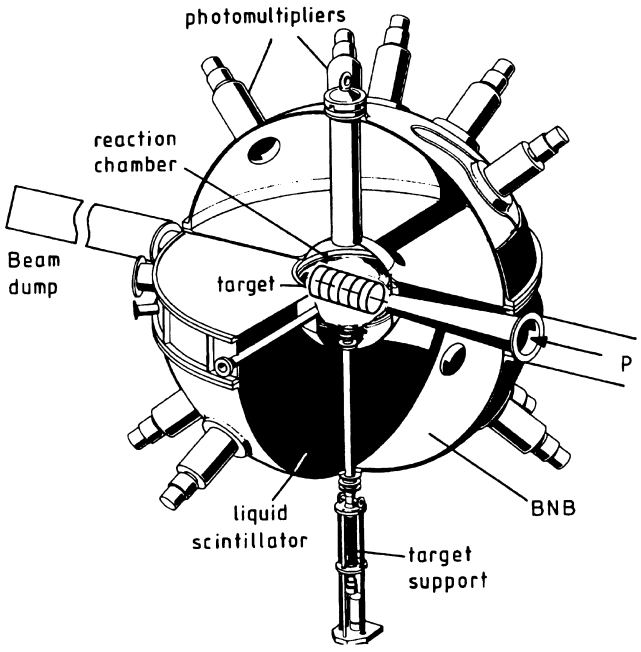

Figure 1.12: The 4π BNB detector with targets stacked in the reaction chamber (taken from [32]).

scintillator light is being registered with a set of photomultipliers distributed on the surface of the shell.

Besides multiplicity, an important quantity is the **neutron cost**, i.e., the number of produced neutrons normalized per one incident particle and per unit of its energy. Monte-Carlo simulations of neutron cost on thick, lead target as well as various experimental data show that the optimal proton energy for maximum neutron yield favourable for ADS purposes can be reached around 1 GeV [29], see **Fig. 1.13**.

1.5.2 Target parameters

Regarding target parameters, its material and size are those which determine the neutron multiplicity. In principle, the heavier target nucleus the larger amount of neutrons is being produced. The gain factor between heavy and light targets is around a factor of five [21], however, the radiotoxicity induced in the spallation target could be significantly reduced when using lighter targets [26]. Neutron multiplicity can be increased by using of a fissile material. In addition, important parameters of target material are thermal conductivity, caloric receptivity, melting and boiling points [30].

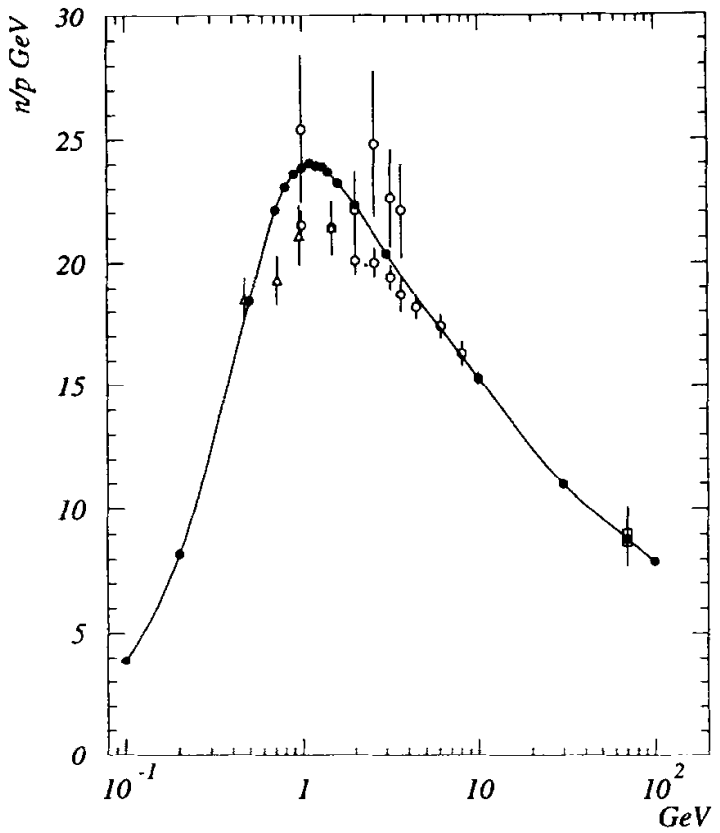

Figure 1.13: Numbers of neutrons with $E_n < 10.5$ MeV (normalized per one incident proton and per unit of proton energy) escaping from the whole surface of the cylindric Pb-target (radius = 10 cm, length = 60 cm) in dependence on the incident proton energy (given in logarithmic scale): full circles represent Monte-Carlo calculations [29], the curve is drawn through the points to guide an eye; open symbols stand for experimental data: triangle [34], circle [35], square [36] - recounted from W to Pb (taken from [29]).

The target should have such a size that at once it incepts the main part of the high-energy cascade and let the spallation neutrons escape. Experiments with different target materials and sizes show that neutron multiplicity saturates at a given target thickness, which increases with the proton energy, see **Fig. 1.14**.

For example, the "saturated thickness" of a thick Pb-target for $\sim$ GeV protons is approximately 100 cm, see **Fig. 1.15**) and "saturated radius" is approximately 50 cm, see **Fig. 1.16**). For such dimensions, a complete saturation of neutron production occurs – it means that it is possible to reach the maximal number of the produced neutrons for the given beam energy,

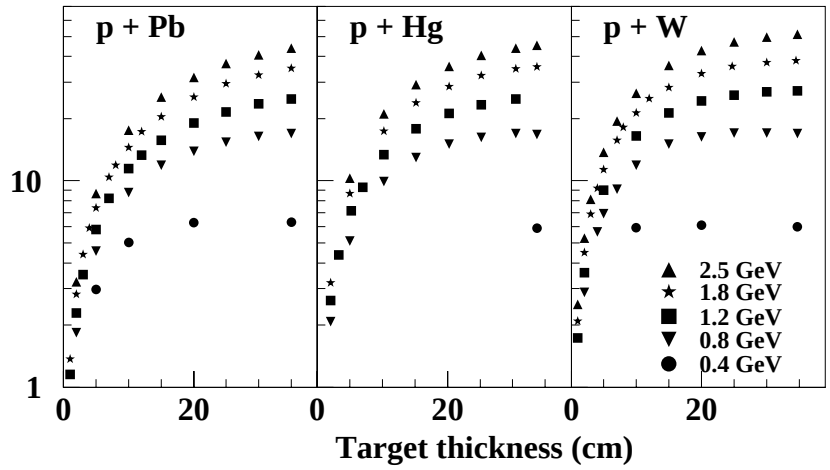

Figure 1.14: Neutron multiplicity as a function of target thickness and beam energy for Pb, Hg, W target materials. All targets were 15 cm in diameter (taken from [32]).

see **Fig. 1.17**.

The saturated thickness is smaller than one could expect considering the electronic-stopping range done by ionization (**Fig. 1.17**), which is bigger than 100 cm even for $E_{\mathrm{p}} > 1.7$ GeV on Pb-target. Saturation is for lower beam energies done by ionization, for bigger energies by loss of protons by nuclear reactions.

The reason consists in practical extinction of the primary proton beam (with the incident energy in a GeV range) before 100 cm of target thickness, because almost all beam particles interact by spallation reactions during this distance. Taking into account that the total reaction cross-section for p+Pb is approximately constant in a GeV-range ($\sigma_{\mathrm{tot}} \approx 1.8$ b, see **Fig. 1.17** right), only 0.3% of the primary proton beam remains after passing 100 cm of lead.

The situation for uranium is different than for lead, because ^{238}U has huge neutron capture cross-section, see **Fig. 1.18**. The U-target size for which the neutron *production* reaches saturation (and for bigger size stays the same) exists too (**Fig. 1.19** left). But important is other size – such, for which the number of *escaped* neutrons (i.e., available for other, for example transmutation, purposes) reaches its maximum (**Fig. 1.19** right) and for bigger target size decreases because of neutron *capture* (see **Fig. 1.20**). The "classical" saturation occurs for radius smaller than 20 cm, where the number of produced neutrons increases more steeply with target thickness than the number of absorbed neutrons. The maximal number of escaped neutrons

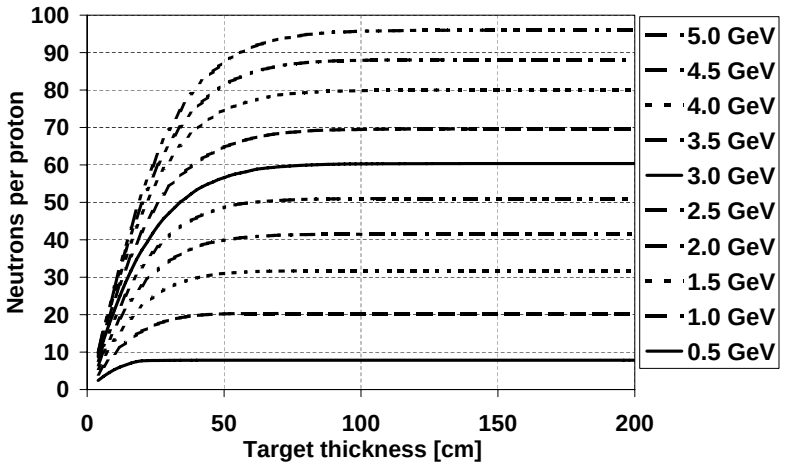

Figure 1.15: Dependence of neutron multiplicity on target thickness and beam energy for a Pb-target with radius of 5 cm (usual radius). MCNPX simulation (Bertini+Dresner). Such dependence was investigated experimentally by Letourneau et al. [32], see **Fig. 1.14**.

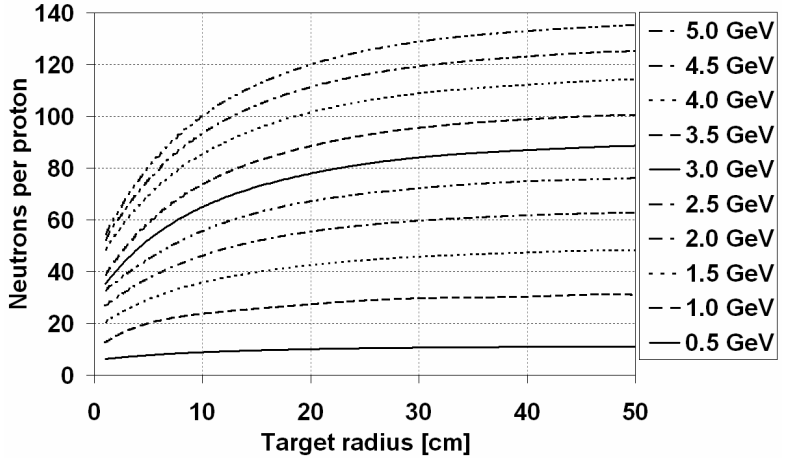

Figure 1.16: Dependence of neutron multiplicity on target radius and beam energy for a Pb-target with thickness of 100 cm (saturated thickness). MCNPX simulation (Bertini+Dresner).

happen for $R \approx 20$ cm, $L \approx 100$ cm. For bigger target radii the number of escaped neutrons drops as the number of captured neutrons increase.

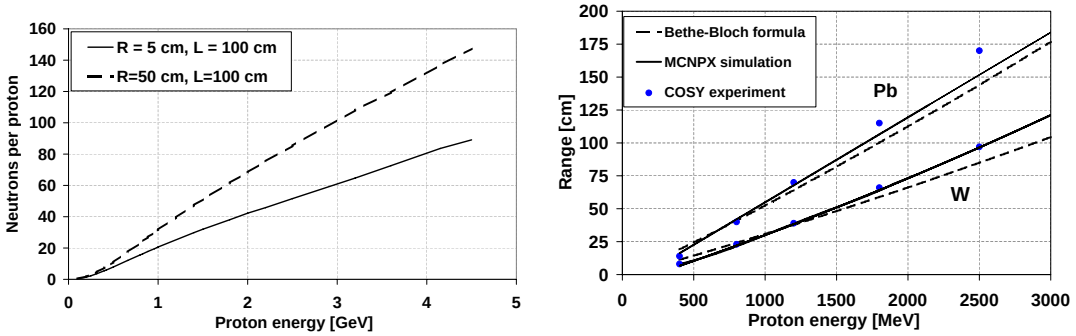

Figure 1.17: Left: Dependence of neutron multiplicity produced on a Pb-target with radius of 5 cm (usual radius) and 50 cm (saturated radius), both for target thickness of 100 cm (saturated thickness), on proton beam energy. MCNPX simulation.
Right: Range of protons in tungsten and lead. Various sources: Bethe-Bloch formula [31], MCNPX simulation (author's simulations), experiments of the NESSI collaboration [32].

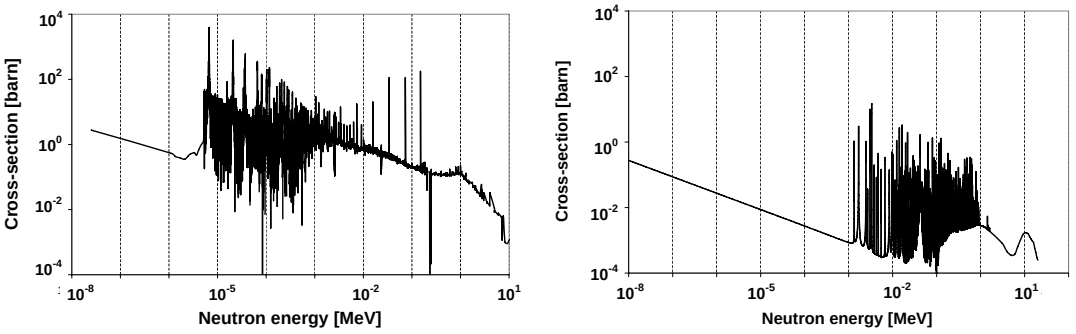

Figure 1.18: Neutron capture cross-section on ^{238}U [37] (left) and ^{nat}Pb [38] (right).

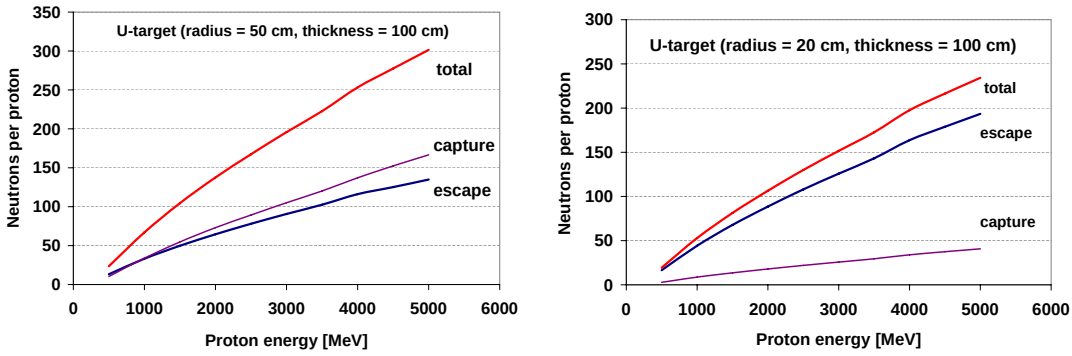

Figure 1.19: Dependence of neutron multiplicity on beam energy for a U-target. Two important cases are plotted: saturated target size for maximal neutron production – radius of 50 cm, thickness of 100 cm (left); optimal target size for maximum number of escaped neutrons – radius of 20 cm, thickness of 100 cm (right). MCNPX simulation (Bertini+Dresner).

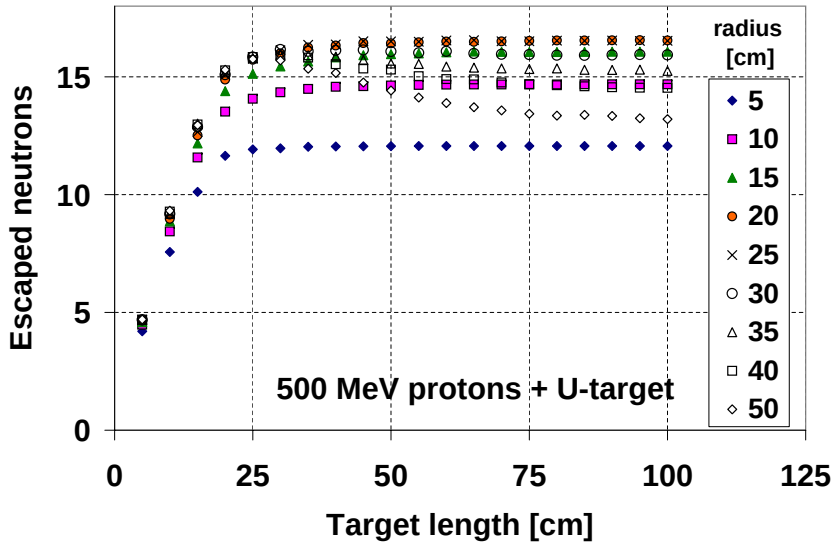

Figure 1.20: Numbers of neutrons escaped from surface of a U-target irradiated with the 0.5 GeV proton beams in dependence on target size. MCNPX simulation (Bertini+Dresner).

Chapter 2

Spallation experiments

The ADS principle based on a subcritical nuclear reactor driven by an external spallation neutron source was designed to produce fissile material and has already been suggested in the late 1940's.

The production of large amounts of neutrons by high-power accelerators became possible after the Lawrence's invention of a cyclotron in 1929. After participating the Manhattan Project, E. O. Lawrence brought in the idea of the accelerator as a neutron source with the intention to produce fissionable material. His MTA project (Materials Testing Accelerator) began at the Lawrence Livermore National Laboratory in California in 1950 [39]. He proposed to irradiate various thick targets (U, Be, Li) by protons and deuterons to measure the cross-sections, neutron yields, and the feasibility of converting the fertile (depleted uranium or thorium) to fissile material (^{239}Pu, ^{233}U). This was the first motivation, because the USA were dependent on foreign uranium sources. The MTA project was closed a few years later when rich domestic uranium ores were found in the Colorado plateau.

During next decades, investigations important for the estimation of efficiencies of various modes of transmutation were performed. For example, neutron yields and spectra in lead and uranium targets irradiated by relativistic protons [27, 40] and nuclei [41] and neutron cross-sections for a number of isotopes have been measured in JINR Dubna.

The first quite conceptual and complex study of the radioactive waste transmutation has started at the end of 1980's at JAERI (Japan Atomic Energy Research Institute). A long-term program for research and development on nuclide partitioning and transmutation technology was called OMEGA [42] (Option Making Extra Gains from Actinides and Fission Products). This program initiated the global interest in transmutation topic that started from the beginning of 1990's.

At that time, two main projects have been published. C. Bowman from

LANL (Los Alamos National Laboratory) created a detailed concept of the **Accelerator Transmutation of Waste** (ATW) [6] using *thermal* neutrons. He suggested the use of a linear accelerator with a high-intensive proton current ($\sim$ 250 mA) of 1.6 GeV energy.

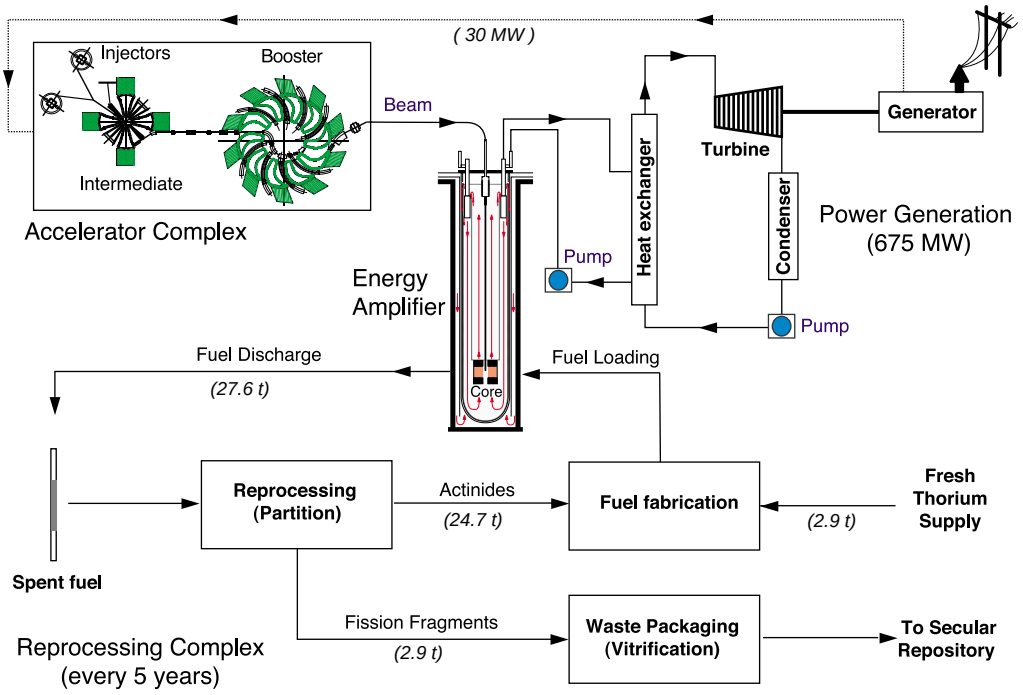

Figure 2.1: General lay-out of the Energy Amplifier complex. The electric power generated is used to run the accelerator (re-circulated power estimated to $\leq 5\%$). At each discharge of the fuel (every five years) the fuel is "regenerated". Actinides (mostly Th and U) are re-injected as new fuel in EA, topped with fresh Th. Fission fragments and the like are packaged and sent to the secular repository, where after ≈ 1000 years the radioactivity decays to a negligible level (taken from [44]).

C. Rubbia from CERN (Conseil Européen pour la Recherche Nucléaire = European Council for Nuclear Research) proposed a basic concept of the **Energy Amplifier** [43], also called **Accelerator Driven Energy Production** (ADEP), see **Fig. 2.1**. As the name implies, it does not pay interest to the disposal of radioactive waste directly. The motivation for ADEP is similar as for the MTA project. This idea is based on the use of thorium[1] as

[1]Thorium is about three times more abundant element in the earth's crust than uranium. Particularly, India and Australia, thanks to their large reserves of thorium, plan to base their nuclear power programs on thorium [45].

a fuel for the production of fissile ^{233}U:

$$\mathrm{n} + {}^{232}\mathrm{Th} \xrightarrow{\gamma} {}^{233}\mathrm{Th} \xrightarrow[22\ \mathrm{m}]{\beta^-} {}^{233}\mathrm{Pa} \xrightarrow[27\ \mathrm{d}]{\beta^-} {}^{233}\mathrm{U}.$$

It reckons with a use of a 1 GeV cyclotron with smaller beam current than in LANL (12.5 mA) for transmutation by *fast* neutrons. In the case of using the Energy Amplifier for waste transmutation, the fast neutrons could fission all higher actinides, while the thermal neutrons in a classical nuclear reactor do not fission many of them.

A lot of projects all around the world have been established to carry out experiments for nuclear data acquisition, complement of cross-section libraries, testing the accuracy of models describing spallation and transmutation reactions. The aim of such investigations is to design the optimal parameters of accelerator, beam, target, and blanket. The main projects in European scale are following.

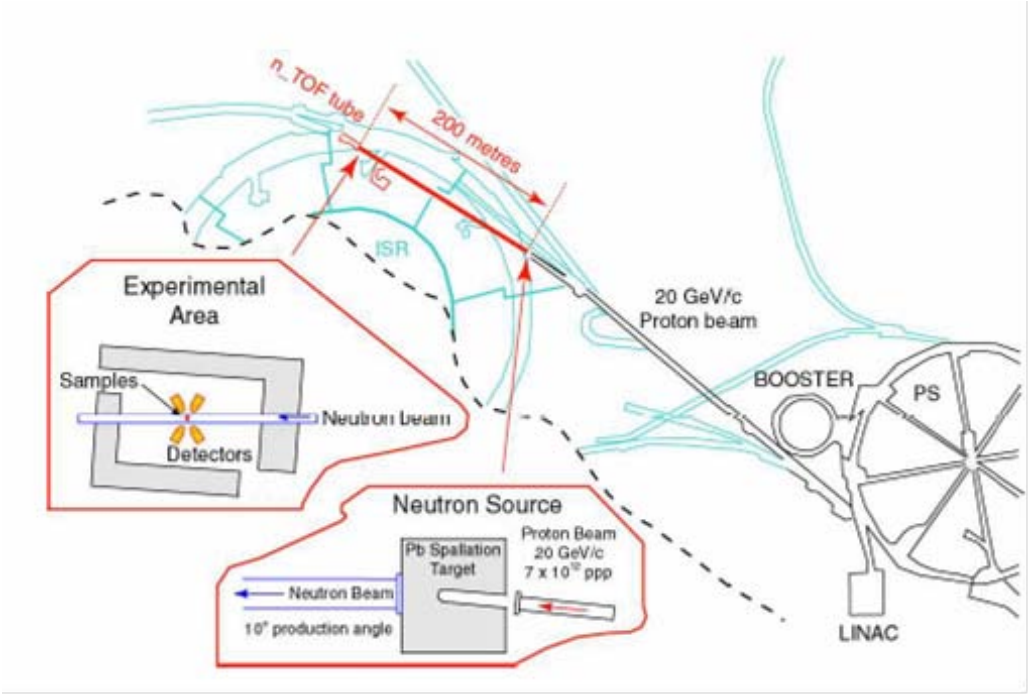

Figure 2.2: General layout of the nTOF experiment. The proton beam was extracted via the TT2 transfer line and hit the Pb-target. At the end of the TOF tunnel (TT2-A), neutrons were detected about 185 m from the primary target (taken from [48]).

- n_TOF (neutron Time-Of-Flight measurements) [49] in CERN was project focused on cross-sections measurements of neutron capture and fission on minor actinides, neutron capture on fission products, and (n,xn)-reactions on structural and coolant materials, which are supposed to be used in ADS. It used proton beam with the momentum of 20 GeV/c and the intensity of 7×10^{12} protons per pulse (with the repetition frequency of 2.4 Hz) hitting a Pb-target with the dimensions of $80 \times 80 \times 60$ cm^3, see **Fig. 2.2**.

- MEGAPIE (Megawatt Pilot Target Experiment) [52] in PSI (Paul Scherrer Institut) in Switzerland was project to demonstrate the feasibility of a liquid Pb+Bi eutectic target for high-power ADS applications. It operated (in 2006) with 590 MeV proton beam with an average current of 1.3 mA corresponding to a beam power of 0.77 MW. One of the results was about 80% more neutrons compared to previously operated Pb-target.

- HINDAS (High and Intermediate energy Nuclear Data for Accelerator-driven Systems) [61] was a joint European program designed to gather nuclear data for transmutation in the 20-2000 MeV range with focuse on typical materials for construction (Fe), target (Pb), and core (U). It used six facilities throughout Europe during 2000-2003; for an example of the results see **Fig. 1.4**.

- FEAT (First Energy Amplifier Test) [50] in CERN was an experiment for studying the energy amplification in ADS, defined as the ratio between the energy produced in ADS and the energy provided by the beam. It was shown that the energy gain is independent on the proton beam intensity and the beam kinetic energy for $E_\mathrm{p} > 900$ MeV.

- TARC (Transmutation by Adiabatic Resonance Crossing) [51] in CERN was an experiment whose main purpose was to demonstrate the possibility of using Adiabatic Resonance Crossing to destroy efficiently long-lived fission fragments in ADS. It was studied how spallation neutrons slow down quasi-adiabatically with almost flat iso-lethargic energy distribution and reach the capture resonance energy (of an element to be transmuted) where they have high capture cross-section.

- SPALADIN (Spallation based on A Large Acceptance DIpole magNet) in GSI in Germany [59] is an experiment to study the spallation of ^{56}Fe at 1 AGeV in inverse kinematics, see **Fig. 2.3** (iron is the main structural component of ADS, in particular for the vacuum window

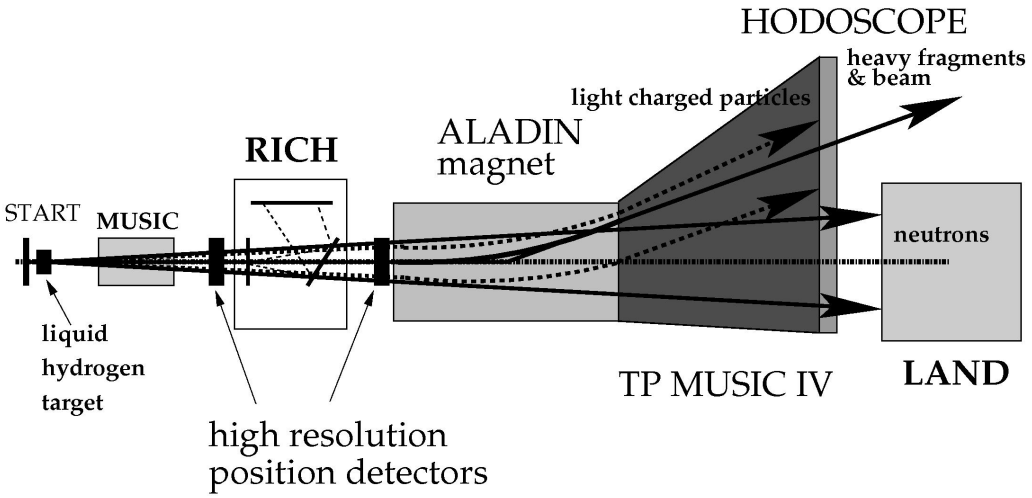

Figure 2.3: General layout of the SPALADIN experiment in GSI Darmstadt (taken from [59]).

in between the spallation target and the proton accelerator). One of the interesting results are spallation residues far from the projectile, which show that the nucleus de-excitation does not simply consist in light-particle emission.

- MUSE (MUltiplication Source Externe) [54] was a series of experiments in CEA-Cadarache in France during 1995-2003. The general purpose was to study the behaviuor of subcritical systems coupled with an accelerator. The studies were conducted in a low power mock-up (< 5 kW) of a subcritical assembly, where temperature effects are negligible. The mock-up was coupled to a well-calibrated external neutron source.

- YALINA [60] in Minsk, Belarus is a subcritical uranium-polyethylene target-blanket assembly operating with a thermal neutron energy spectrum provided by a $100 - 250$ keV deuteron beam ($1 - 12$ mA) on a tritium target. Its main purpose is to study neutron physics of ADS.

- TRASCO (TRAsmutazione SCOrie) [56] in Italy was a project to study physics and develop technologies needed to design ADS. It operated a 40 mA proton beam and Pb-Bi target.

- TRADE (TRiga Accelerator Driven Experiment) [55] in the ENEA-Casaccia Centre in Italy is a project (currently stopped) based on the coupling of a proton cyclotron with a solid Ta-target, surrounded by a

reactor core in a subcritical configuration based on the TRIGA (Training, Research, Isotopes, General Atomics) reactor.

- MYRRHA (Multi-purpose hYbrid Research Reactor for High-tech Applications) [57] in SCK-CEN (Studiecentrum voor Kernenergie – Centre d'Étude de l'énergie Nucláeaire) in Belgium is a project to built a demonstration ADS. High intensive 2.5 mA proton beam with the energy of 600 MeV (1.5 MW) will irradiate a liquid Pb-Bi target with a subcritical MOX blanket (30% Pu) with $k_{\text{eff}} = 0.95$. MYRRHA will be a fast neutron facility for studies of transmutation of minor actinides, material development for Gen-IV systems and fusion reactors. It will also allow radioisotope production for medical and industrial applications. It is currently planned to be in full operation by 2020 [58].

One of such places, where the investigation of ADS has been intensively carried out is also JINR Dubna. Currently, several directions of this research are being evolved there, see next four sections.

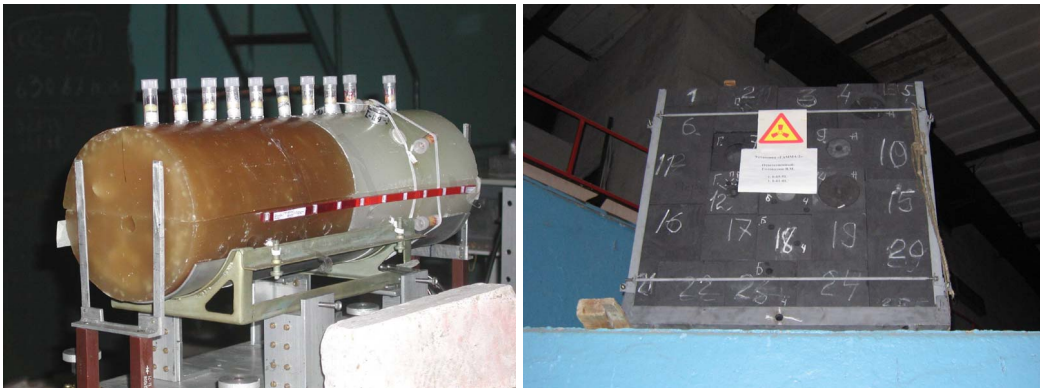

Figure 2.4: Photos of the Gamma-2 setup with La-sensors on the top of the paraffine moderator (left) and the new Gamma-MD setup (right).

2.1 The Gamma project

The Gamma project is an instrument to study spallation neutron production by GeV protons on a thick, heavy target and the influence of moderator on the produced neutron field [62]. The setup consists of a thick target (Pb, U) of the diameter $d = 8$ cm and the length $l = 20$ cm surrounded by moderator. Until now, several experiments have been carried out with the

paraffine moderator of the thickness of 6 cm (Gamma-2 setup). It is the best possible moderator, but technically useless because of low melting point and flammability.

The first experiment on the new setup called Gamma-MD (M stands for Minsk, D stands for Dubna) with the Pb-target of the length $l = 60$ cm and graphite moderator (technologically usable) of a cubic size ($110 \times 110 \times 60$ cm^3) was carried out in March 2007 with 2.33 AGeV deuteron beam.

The low-energy neutron spatial distribution is being measured by the activation sensors of ^{139}La with (n,γ)-reaction. Transmutation of higher actinides and fission products in moderated neutron field is also being studied [63]. Thanks to the simple setup geometry, the experimental results from Gamma-2 and Gamma-MD experiments are useful for testing the accuracy of high-energy codes (see chapter 3).

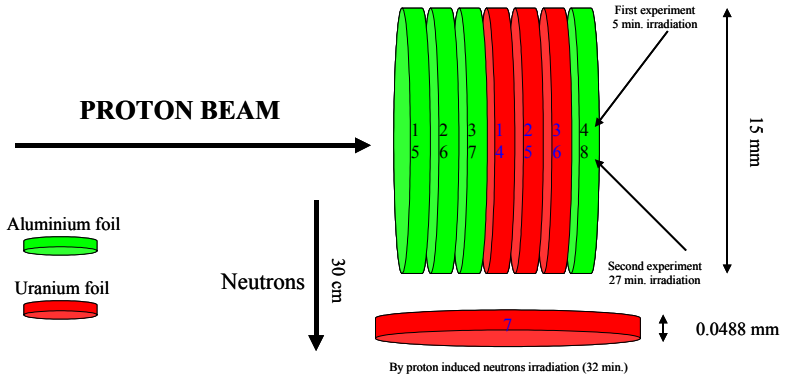

Figure 2.5: Measurements of the cross-sections of $^{\rm nat}$U(p,$xpyn$)$^{\rm A}_{\rm Z}$Res on direct proton beam from the Phasotron. Al-folis were used for beam monitoring (taken from [64]).

2.2 The cross-sections measurements

The Phasotron accelerator is being used to study the cross-sections of the proton reactions ($E_{\rm p} = 660$ MeV) on thin targets of fission products (^{129}I), natural uranium [64], and higher actinides (^{237}Np, ^{241}Am [65], ^{239}Pu). Thanks to the usage of direct kinematics technique (see **Fig. 2.5** and section 1.3), many isotopes produced with wide spectrum of half-lives (from minutes until years) have been observed. The comparisons with computer codes have been performed [66] to check the theoretical models. The plan is to continue in the cross-section measurements and to carry out experiments with ^{232}Th, ^{238}Pu, ^{235}U.

2.3 The SAD project

The SAD project [67] is a plan to construct the facility consisting of a replaceable spallation target (Pb, W) with a subcritical MOX blanket (UO_2 + PuO_2), using also the Phasotron accelerator, see **Fig. 2.6**. The motivation is to study the neutron production in such a setup (spectral and angular flux distributions), prompt neutrons life-time, effective fraction of the delayed neutrons, spallation product yields, power release, fission rates of actinides, transmutation rates of fission products, shielding efficiency, and accuracy of the computer codes and the nuclear databases used for calculations of the ADS characteristics. Final design is not given yet, preparation of equipments and theoretical calculations of the setup parameters are in progress [68]. The technical realization of the project was held up when Sweden withdrew from the contract.

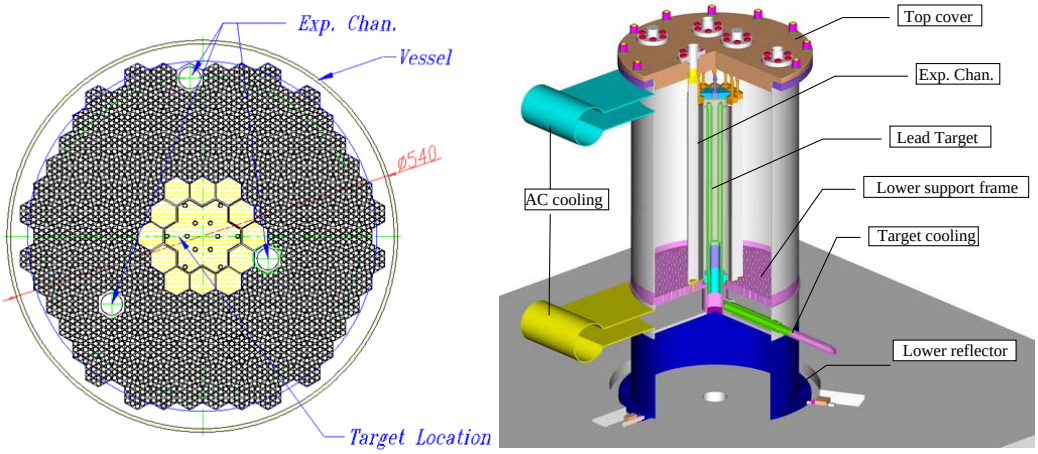

Figure 2.6: A cross section of the SAD active core (left) and a general view of the SAD core (taken from [68]).

2.4 Energy plus Transmutation

"Energy plus Transmutation" (E+T) is a wide international collaboration (scientists from Armenia, Australia, Belorussia, the Czech Republic, Germany, Greece, India, Mongolia, Poland, Russia, Serbia, Ukraine). It uses the setup of the same name (**Fig. 2.7, 2.8**) consisting of a 28.66 kg thick lead target with a 206.4 kg deep-subcritical ($k_{\text{eff}} = 0.202$ [96]) natural uranium blanket surrounded by a polyethylene shielding (the whole assembly mass is

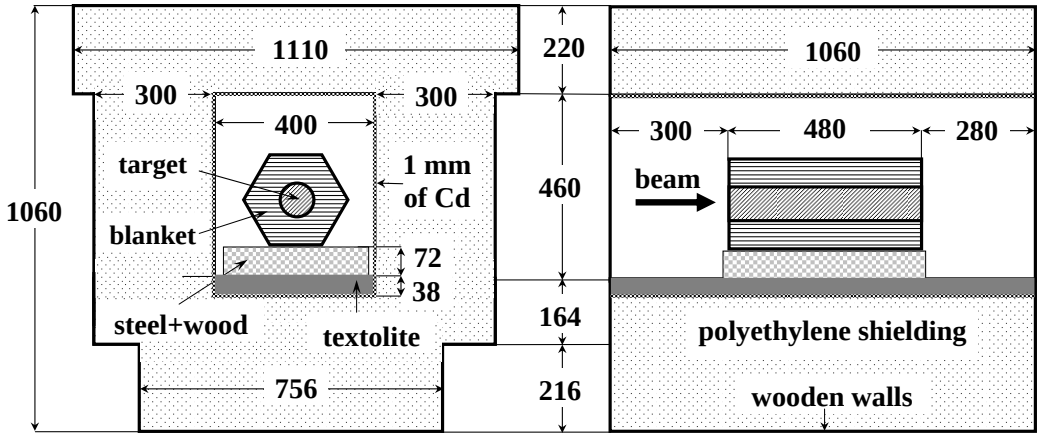

Figure 2.7: Front view (left) and cross-sectional side view (right) of the "Energy plus Transmutation" setup. Dimensions are in millimeters.

950 kg). The complex investigation within the frame of the E+T project pursues:

- transmutation of fission products and higher actinides (refined from burned-up nuclear fuel) by spallation neutrons [69, 70, 71, 72, 80, 81, 82];
- the spatial and energetic distributions of spallation neutrons by the activation analysis method using Al, Au, Bi, Co, Cu, Dy, Fe, In, La, Lu, Mn, Nb, Ni, Ta, Ti, and Y sensors (neutron capture for thermal, epithermal, and resonance component, threshold reactions for fast component of neutron spectra) [84, 87, 90, 92, 95], solid state nuclear track detectors [73, 74, 75], nuclear emulsion techniques [76], and He-3 proportional counters [77];
- tests of the accuracy of the computer codes for calculation of neutron spectra and transmutation yields [86, 91, 94].

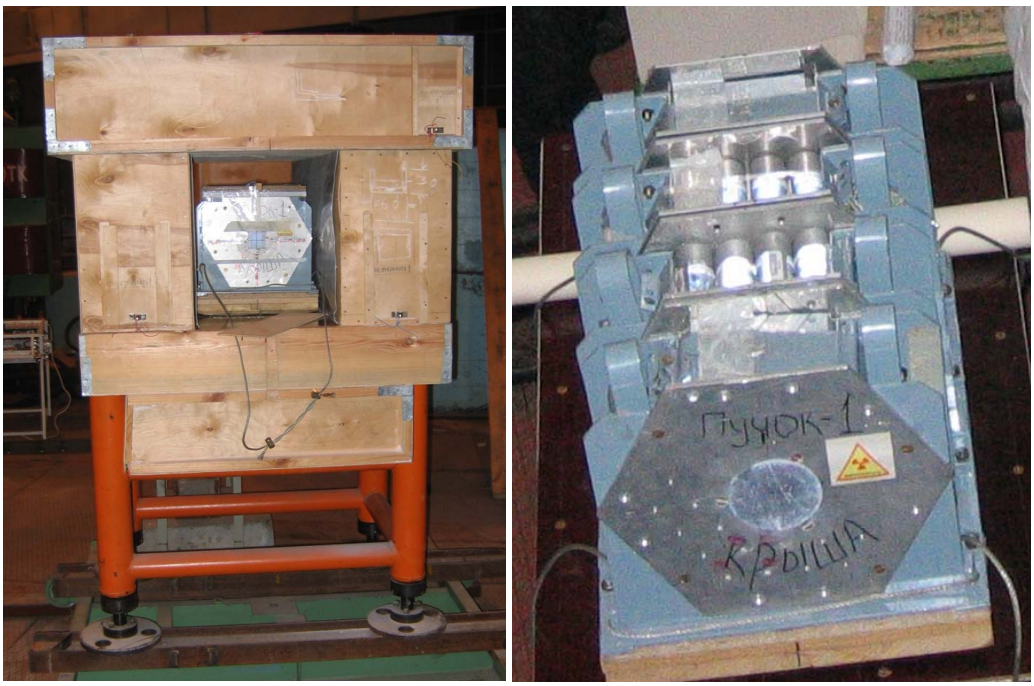

Figure 2.8: Photos of the "Energy plus Transmutation" setup (left) and the Pb/U–target/blanket assembly (right).

Chapter 3

Simulations of high-energy nuclear reactions

As mentioned in the previous chapter, there is a strong need of simulation codes for ADS assembly projection. Several simulation codes and combinations of these codes exist. They describe spallation reactions, interactions of secondary particles, and the following neutron transport through the target material, e.g.:

- LAHET (Los Alamos High Energy Transport Code) [98] can model spallation reactions and transport of nucleons, pions, muons, antinucleons with the energy $E \geq 20$ MeV. LAHET generates cross-sections for individual processes;
- MCNP (Monte Carlo N-Particle Transport Code) [99] is able to model the transport of neutrons (and photons and electrons) in an energy range 10^{-11} MeV $\leq E \leq 20$ MeV. It uses libraries of evaluated data as a source of the cross-sections;
- MCNPX (MCNP eXtended) code [100] improves and links the advantages of both LAHET and MCNP. MCNPX has been under continuous development since 1994 and it was first released to the public in 1999 as version 2.1.5 [117]. MCNPX supports 34 particle types, the ability to calculate interaction probabilities directly with physics models for energies where tabular data are not available;
- FLUKA (FLUktuirende KAskade) [102],
- HETC (High Energy Transport Code) [103],
- NMTC (Nucleon Meson Transport Code) [104],

- NUCLEUS [139],
- SHIELD [106],
- CASCADE [107],
- CEM (Cascade-Exciton Model) [108],
- GEM (Generalized Evaporation Model) [110],
- LAQGSM (Los Alamos Quark-Gluon String Model) [109],
- GEANT4 [111],
- JAM (Jet AA Microscopic Transport Model) [112],
- MARS [113],
- TIERCE [114],
- BRIEFF [115].

They are based on the *mathematical* Monte-Carlo method and they use various *physics* models of spallation reactions and cross-section libraries of neutron-induced reactions.

3.1 The Monte-Carlo method

The Monte-Carlo method [116] is a numerical technique used for simulating the behavior of various systems (from economics to particle physics) more complex than we otherwise can. In contrast to deterministic algorithms (used by other codes, section 3.4), it is a stochastic method. It is based on an executing of many random experiments (with a model of a system). The essential point is to have a high-quality generator of pseudo-random numbers (it is not necessary to use really random numbers). The result is a probability of some effect.

In particle reaction and transport tasks, individual particles trajectories are being simulated. To determine if an event occurs, the probabilities of possible physics processes (i.e., cross-sections) are used and random numbers are generated depending on the probability distributions for every case. The result of the particle life (so-called history) is being stored for the following assessment of average particle behaviour.

The statistical accuracy of results depends on the number of trials given to the simulation. The statistical error approximately matches inverse square

root of the number of histories. That means, to reduce the error by a factor of two, the number of histories must quadruplicate. Accurate enough results for complex ADS systems are achievable in reasonable time thanks to the use of fast parallel computers, which can generate many events simultaneously [88].

3.2 Simulation of stages of spallation reaction

Simulations described in this book were performed using the MCNPX code (an example of a MCNPX input file can be found in Appendix A). MCNPX simulation of spallation reaction consists of three stages (see also section 1) and for each of them a special model is used. The first stage is the Intra-Nuclear Cascade (INC) on which a pre-equilibrium stage concurs. This is followed by an equilibrium evaporation that competes with a fission channel (fission fragments undergo an evaporation stage that depends on their excitation energy). After evaporation, a de-excitation of the residual nucleus follows, generating gammas. MCNPX enables to choose different models for description of individual stages of the spallation reaction.

3.2.1 Intra-nuclear cascade models

INC models (Bertini [118], Isabel [119], CEM [108], INCL4 [120]) describe interactions between an impinging particle and target nucleons during intra-nuclear cascade as a sequence of binary collisions separated in space and time. This is valid if the incident particle wavelength is smaller than a mean distance between nucleons of the target nucleus, thereto, a mean free path of the incident particle in the target nucleus is greater than the inter-nucleon lengths. The trajectory between collisions is assumed to be linear.

The collisions proceed until a certain degree of equilibrium is reached. The criterion used in the INC model of Cugnon (INCL4) is an empirical time of equilibrium (so-called cutoff time $t_{\mathrm{cut}} \approx 30$ fm/c [121] that allows five sequential nucleon-nucleon interactions on the average), which was deduced from a clear change of the calculated quantities (like the integral number of emitted particles, their total kinetic energy or the excitation energy of the residual nucleus).

In the Bertini-type model (Bertini, Isabel) the equilibrium criterion is deduced from the energy of the fastest particle remaining in the nucleus (so-called cutoff energy T_{cut}), which should be smaller than the nuclear potential well depth (≈ 40 MeV [15]).

The CEM code uses a criterion for the escape of a primary particle from the cascade stage via the effective local optical potential $W_{\mathrm{opt.mod}}(r)$ deter-

mined from the local interaction cross-sections, including the blocking effects due to the Pauli exclusion principle. This imaginary potential is compared with "experimental" potential $W_{\mathrm{opt.exp}}(r)$ determined in terms of the phenomenological global optical model by using data on elastic scattering by a nucleus. The convergence degree of imaginary potentials is determined via the parameter $P = |(W_{\mathrm{opt.mod}}(r) - W_{\mathrm{opt.exp}}(r))/W_{\mathrm{opt.exp}}(r)|$. If P exceeds an empirically selected value (≈ 0.3), the particle escapes from the cascade stage, becoming an exciton. With the selected P-value, the cascade part of the code becomes shorter than in other cascade models [122].

The nuclear density distribution is approximated by a step-function distribution (as a function of target radius), where the densities in regions with constant density (three for Bertini, seven for CEM03, 16 for Isabel) are fitted to the folded Saxon-Woods shape. In INCL4, the Saxon-Woods density distribution is used and cut at the radius described with a diffuseness parameter. Fermi motion of the nucleons and the quantum effects of Pauli blocking are taken into account. High-energy parts above the range of INC physics usability are taken from FLUKA [102].

3.2.2 Pre-equilibrium models

Pre-equilibrium models (Multistage Preequilibrium Exciton Model [123], Modified Exciton Model [124]) describe the process of energy equalization as a sequence of two-particle interactions, whereas the nucleus is, in each phase (i.e., after each interaction), defined as the number of particles and vacancies. This description of a nucleus is called the exciton model, see **Fig. 3.1**. An exciton is either a nucleon excited above the Fermi level or a vacancy under the Fermi level.

The exciton model solves the master equation[1] describing the equilibration of the excited residual nucleus that remains after the cascade reaction stage. While, the master equation of MPM neglects angular distributions of pre-equilibrium particles, MEM includes momentum and angular momentum conservations of the nuclear system at the pre-equilibrium and equilibrium evaporation stages. MPM considers only nuclear transitions in the direction of equilibration (change of $\Delta n = +2$ in the exciton number). MEM takes into account all possible nuclear transitions ($\Delta n = +2, -2, 0$), considering all possible positions of particle-hole pairs with respect to the Fermi level ($\Delta n = 0$).

[1] A master equation is a phenomenological set of first-order differential equations describing the time evolution of the probability of a system to occupy each one of a discrete set of states.

The nucleus comes near to the equilibrium particle-whole configuration with each interaction of incident or cascade particle with other nucleons. When the equilibrium state is reached, the pre-equilibrium model is replaced by evaporation model.

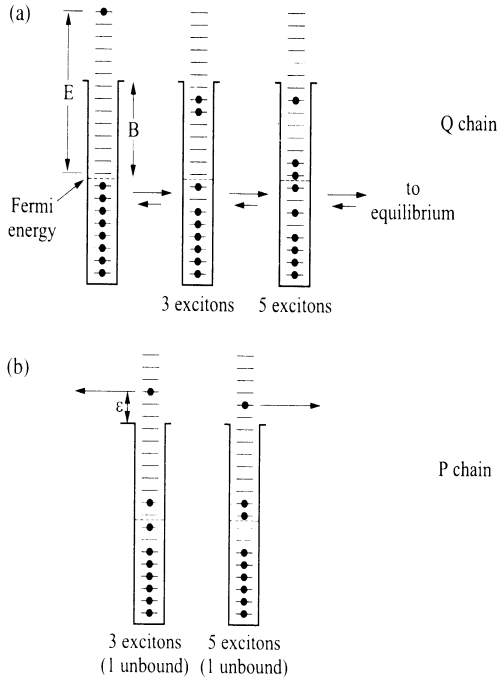

Figure 3.1: Schematic representation of the first few stages of a nucleon-induced reaction in the exciton model. The horizontal lines indicate equally spaced single-particle states in the potential well. The particles are shown as solid circles. E is the incident particle energy measured from the Fermi level, B is the average nucleon binding energy.
Part (a) shows nucleon-nucleon interactions leading to more complex configurations, in which all particles are bound and cannot be emitted.
Part (b) shows interactions leading to configurations, in which at least one particle is unbound and may be emitted with the energy ε leaving a residue with the energy $U = E - B - \varepsilon$.

3.2.3 Evaporation and fission models

Evaporation models (Dresner [125], ABLA [126]) describe the equilibrium decay of an equilibrium nucleus with the excitation energy reached at the end of the pre-equilibrium stage. The probability of the nucleus decay into

a certain channel depends on level densities in a final channel and on the probability of a passage through the energy barrier.

As a competitive process to equilibrium decay, high-energy fission can happen. MCNPX includes two models of residual nuclei fission: ORNL (Oak Ridge National Laboratory) model [127] for actinides with $Z \geq 91$ and RAL (Rutherford Appleton Laboratory) model [128] which covers fission of actinides and subactinides with $Z \geq 71$.

3.3 Nuclear data libraries

EXFOR (Experimental Nuclear Reaction Data) [37] is a database containing experimental data, their bibliographic information, experimental information, and source of uncertainties.

Through the process of critical comparison, selection, renormalization, averaging of experimental data and completion by nuclear model calculations, evaluated data libraries are being produced. They are normally stored in a computer readable format called the ENDF format [131]. General purpose evaluated libraries are:

- ENDF/B-VII.0 (USA, 2006) - Evaluated Nuclear Data File [38],
- JEFF-3.1 (Europe, 2005) - Joint Evaluated Fission and Fusion File,
- JENDL-3.3 (Japan, 2002) - Japanese Evaluated Nuclear Data Library,
- BROND-2.2 (Russia,1992),
- CENDL-2 (China,1991) - Chinese Evaluated Nuclear Data Library.

Besides general libraries, a large number of special purpose evaluated data libraries exist, e.g.:

- WIND (Waste Incineration Nuclear Data library), MENDL (Medium Energy Nuclear Data Library) - (both Obninsk, Russia) - neutron reaction data libraries for nuclear activation, transmutation, threshold reactions and fission up to 100 MeV;
- LA150 [129] (LANL, USA) - cross-section library of evaluated neutron and proton cross-sections up to 150 MeV, which have been developed using experimental data as well as nuclear reaction models in the GNASH code [144]. LA150 includes evaluations for the major isotopes of structural, shielding, and target-blanket importance: H, Li, C, N, O, Al, Si, P, Ca, Fe, Ni, Cr, Cu, Nb, W, Hg, Pb, Bi [132];

- NRG-2003 [130] (the Netherlands) - cross-section library up to 200 MeV has been evaluated using mainly the TALYS code [141]. NRG-2003 includes evaluations for: Ca, Sc, Ti, Fe, Ni, Pb, Bi [133]).

3.4 Deterministic codes

Deterministic codes are based on the solution of neutron transport equations. Several "all-in-one" deterministic nuclear reaction codes have been developed, e.g.:

- TALYS [141] is a nuclear reaction code created at NRG Petten, the Netherlands, and CEA Bruyères-le-Châtel, France. It is able to simulate nuclear reactions in the 1 keV – 250 MeV energy range involving n, p, d, t, helions, α, and γ (as projectiles and ejectiles), and targets with mass numbers between 12 and 339. It incorporates nuclear models for the optical model, level densities, direct, compound, pre-equilibrium, and fission reactions, and a large nuclear structure database. It calculates total and partial cross-sections, energy spectra, angular distributions, double-differential spectra, residual production cross sections, and recoils [142]. It has been tested with experimental data with very good results [143]. The TALYS input file consists of keywords and their associated values, an example can be found in Appendix B.

- GNASH [144] - provides a flexible method by which reaction and level cross sections, isomer ratios, and emission spectra can be calculated;

- ALICE/ASH [145] - calculates multiple particle emission, evaporation including fission competition, pre-compound decay, single and double differential spectra, and reaction product cross sections;

- STAPRE [146] - calculates energy-averaged cross sections for nuclear reactions with emission of particles, γ-rays, and fission;

- EMPIRE [147] - calculates isomer ratios, residue production cross-sections, emission spectra. Incident particle can be any nucleus.

3.5 Validation and verification of high-energy nuclear models

The state-of-the-art of the predicting capabilities of high-energy nuclear models is being studied by the comparisons between models and experimental

data.

The total neutron production, which is of major importance for applications, can be predicted with a precision of $10-15\%$ [134] with any combination of intra-nuclear cascade and evaporation models used in MCNPX. General trends of energy, angular or geometry dependence are also well understood, although, local discrepancies, particularly in the $20-80$ MeV region, may be as large as a factor of 2 or so in extreme cases [134, 135, 136, 137, 138], see examples in **Fig. 1.3, 3.2**.

It is not always easy to determine whether the reason of the observed discrepancies comes from a lack of reliability of data or from faults in models and which part of model could be responsible for that. To solve these problems, more experiments are needed to be carried out very carefully for better understanding of the reaction mechanisms.

Several terms are being use while testing models: validation, verification, benchmark. Validation is the process of checking if some method is correct or is suited for its intended purpose[2]. Verification is the process of checking that a method satisfy the requirements and design specifications[3]. Benchmark experiment is an experiment with the aim of comparing and ranking algorithms with respect to certain performance criterions.

[2]Validation can be expressed by the question "Are you building the right thing?"

[3]Verification can be expressed by the question "Are you building the thing right?"

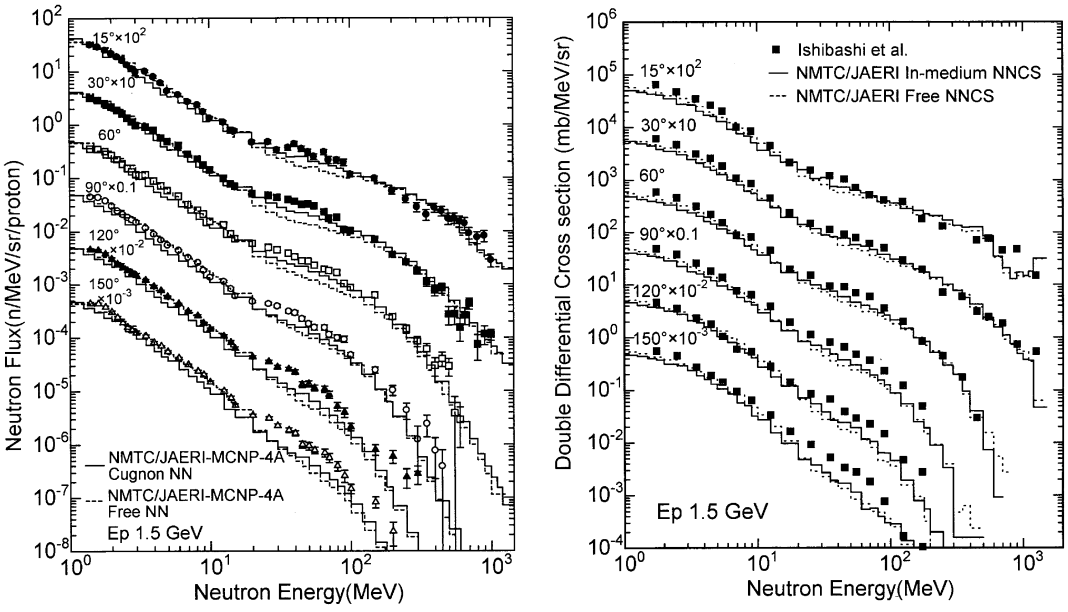

Figure 3.2: Neutron production in reactions of 1.5 GeV protons on a thick (left) and thin (right) Pb-target. Each successive curve is scaled by a factor of 10 with decreasing angle. Symbols indicate experimental data ([137] - left, [136] - right), dashed and solid lines show results of simulations [137].
The simulations underestimate (in comparison with the experiments) the neutron emission at deeper angles. Some studies [139, 140] suggested that the inclusion of the pre-equilibrium process or the refraction and reflection processes improved the backward neutron emission (taken from [137]).

Appendix A
MCNPX input file

MCNPX input file containing all information about the task has three main parts called cards, separated by white lines.

- The Cell Card contains information about the material in the cells, their densities, and the geometry of the cells defined using surfaces.
- The Surface Card defines coordinates of the surfaces in the setup.
- The Data Card contains other parameters of simulation like the cells materials, cross-section libraries, source definition (particle, energy, position, direction, shape), number of the particles to be simulated, and so-called tally cards that specify what type of information the user wants to gain. Tallies are normalized to be per source particle. MCNPX is able to simulate (to tally) current over a surface, flux at a point or over a surface or a cell, energy deposition over a cell, criticality etc.

This is a MCNPX input file describing a cylindrical Pb-target ($r = 5$ cm, $l = 30$ cm) irradiated with a 1.5 GeV proton beam with homogeneous profile and the radius of 1.5 cm. Italic font is used for comments. A slice of the output file follows with indicated information about neutron production.

c CELL CARD
Pb-target
(cell number, material number, density, surfaces numbers – the intersection operator is a blank space between two signed surface numbers)
1 1 -11.340 1 -2 -3
2 0 (-1:2:3) -4
3 0 4

c SURFACE CARD
z planes for target with length of 30 cm
1 pz 0.0
2 pz 30.0
cylinder with radius of 5 cm
3 cz 5.0
4 so 90.0

c DATA CARD
neutrons, protons, photons, charged pions
mode n h p /
particles simulated in all cells
*("n*r*" means repeat the preceding entry on the card n-times.)*
imp:n,h,p,/ 1 1r 0
definitions of materials (material number, 1000·*proton number+nucleon number, nuclide fraction in the material, libraries)*
$^{\mathrm{nat}}Pb$
m1 82204 1.4 82206 24.1 82207 22.1 82208 52.4 hlib=24h nlib=24c cond=1
Neutron physics options
*("n*j*" means jump n-times over the preceding entry and take the default value.)*
phys:n 1500 3j -1
Proton physics options
phys:h 1500 j -1 4j
Photon physics options
phys:p 1500 4j
Pion physics options
phys:/ 1500 4j
INCL4 model
lca 8j 2
ABLA evaporation model
lea 6j 2
the number of incident particles (events)

nps 2e4
homogeneous proton beam with the kinetic energy of 1.5 GeV and the radius of 1.5 cm
sdef par h erg 1500 sur 2 pos 0 0 0 rad d1 dir 1 vec 0 0 1
si1 h 0 1.5
sp1 -21 1

neutron creation	tracks	weight (per source particle)	energy	neutron loss	tracks	weight (per source particle)	energy
source	0	0.	0.	escape	365317	1.8249E+01	2.1995E+02
nucl. interaction	316017	1.5801E+01	3.2136E+02	energy cutoff	0	0.	0.
particle decay	0	0.	0.	time cutoff	0	0.	0.
weight window	0	0.	0.	weight window	0	0.	0.
cell importance	0	0.	0.	cell importance	0	0.	0.
weight cutoff	0	0.	0.	weight cutoff	0	0.	0.
energy importance	0	0.	0.	energy importance	0	0.	0.
dxtran	0	0.	0.	dxtran	0	0.	0.
forced collisions	0	0.	0.	forced collisions	0	0.	0.
exp. transform	0	0.	0.	exp. transform	0	0.	0.
upscattering	0	0.	0.	downscattering	0	0.	9.8498E+00
tabular sampling	0	0.	0.	capture	0	1.4266E-02	7.6455E-02
(n,xn)	78320	3.9123E+00	1.8804E+01	loss to (n,xn)	25352	1.2660E+00	4.8878E+01
fission	0	0.	0.	loss to fission	0	0.	0.
photonuclear	0	0.	0.	nucl. interaction	3668	1.8340E-01	6.1409E+01
tabular boundary	0	0.	0.	tabular boundary	0	0.	0.
(gamma,xn)	0	0.	0.	particle decay	0	0.	0.
adjoint splitting	0	0.	0.				
total	394337	1.9713E+01	3.4016E+02	total	394337	1.9713E+01	3.4016E+02

number of neutrons banked 368985
neutron tracks per source particle 1.9717E+01
average time of (shakes)
escape 5.7458E+00
cutoffs
tco 1.0000E+34

Appendix B
TALYS input file

This is an example of the TALYS input file used in the simulations presented in this thesis. Italic font is used for comments. Then, the calculated cross-sections are plotted and compared with experimental and evaluated cross-sections.

neutron as an incident particle
projectile n
gold as a target element
element Au
197 as a nucleon number
mass 197
the name of file with a list of energies (in MeV) of the incident particle
energy range

Bibliography

[1] Rossi B. *About properties of penetrating, corpuscular radiation at sea level*, Zeitschrift für Physik 82 (1933) 151

[2] Masarik J., Kim K. J., Reedy R. C. *Numerical simulations of in situ production of terrestrial cosmogenic nuclides*, Nuclear Instruments and Methods in Physics Research B 259 (2007) 642-5

[3] Cunningham B. B. et al., Physical Review 72 (1947) 739

[4] Serber R. *Nuclear Reactions at High Energies*, Physical Review 72 (1947) 1114-5

[5] Harvey B. G. *Spallation*, chapter 3 in Progress in Nuclear Physics, Editor O. R. Frisch, Pergamon Press, volume 7 (1959) 90-120

[6] Bowman C. D. et al. *Nuclear energy generation and waste transmutation using an accelerator-driven intense thermal neutron source*, Nuclear Instruments and Methods in Physics Research A 320 (1992) 336-367

[7] Lawrence G. *Transmutation and Energy Production with Power Accelerators* [http://accelconf.web.cern.ch/AccelConf/p95/Articles/fpd/fpd03.pdf]

[8] Carminati F. et al. *An energy amplifier for cleaner and inexhaustible nuclear energy production driven by a particle beam accelerator*, CERN report CERN/AT/93-47(ET)

[9] Mason T. E. et al. *The Spallation Neutron Source: A Powerful Tool for Materials Research*, 33rd ICFA Advanced Beam Dynamics Workshop on High Intensity and High Brightness Hadron Beams. AIP Conference Proceedings, Volume 773 (2005) 21-25

[10] Angelone M., Atzeni S., Rollet S. *Conceptual study of a compact accelerator-driven neutron source for radioisotope production, boron neutron capture therapy and fast neutron therapy*, Nuclear Instruments and Methods in Physics Research A 487 (2002) 585-594

[11] Zeman J. *Reactor Physics I.*, ČVUT 2003 (in Czech)

[12] Friedlander G. et al. *Nuclear and Radiochemistry*, J. Wiley & Sons, New York 1955

[13] Cugnon J. *Cascade models and particle production: A comparison*, University of Liège preprint ULG-PNT-91-6-G (1991); Particle Production in Highly Excited Matter, NATO Science Series B 303 (1993) 271-293. ISBN 0-306-44413-5

[14] Hołyński R. et al. *Multifragmentation of the Pb Projectile at 158 GeV/nucleon in Pb-Pb interactions*, Multifragmentation - Proceedings of the Int. Workshop XXVII on Gross Properties of Nuclei and Nuclear Excitations. Hirschegg, Austria, January 17-23, 1999. Edited by Feldmeier H et al. GSI Darmstadt (1999) 128-134

[15] Adair R. K. *Nuclear Potential Well Depth*, Phys. Rev. 94 (1954) 737-8

[16] Ledoux X. et al. *Spallation Neutron Production by 0.8, 1.2, and 1.6 GeV Protons on Pb Targets*, Physical Review Letters 82 (1999) 4412-5

[17] Titarenko Yu. E. et al. *Experimental and computer simulation study of the radionuclides produced in thin ^{209}Bi targets by 130 MeV and 1.5 GeV proton-induced reactions*, Nuclear Instruments and Methods in Physics Research A 414 (1998) 73-99

[18] Michel R. et al. *Cross sections for the production of residual nuclides by low- and medium-energy protons from the target elements C, N, O, Mg, Al, Si, Ca, Ti, V, Mn, Fe, Co, Ni, Cu, Sr, Y, Zr, Nb, Ba and Au*, Nuclear Instruments and Methods in Physics Research B 129 (1997) 153-193

[19] Enqvist T. et al. *Isotopic yields and kinetic energies of primary residues in 1 A GeV ^{208}Pb+p reactions*, Nuclear Physics A 686 (2001) 481-524

[20] Geissel H. et al. *The GSI projectile fragment separator (FRS): a versatile magnetic system for relativistic heavy ions*, Nuclear Instruments and Methods in Physics Research B 70 (1992) 286-297

[21] Armbruster P., Benlliure J. *Basic Nuclear Data at High and Intermediate Energy for Accelerator-Driven Systems*, NUPECC – Nuclear Science: Impact, Applications, Interactions [http://www.nupecc.org/iai2001/report/A6.pdf]

[22] Henzlova D. et al., *Experimental investigation of the residues produced in the 136Xe+Pb and 124Xe+Pb fragmentation reactions at 1 A GeV*, Submitted to Nuclear Experiment, arXiv:0801.3110v1 [nucl-ex]

[23] Cugnon J., Volant C., Vuillier S. *Nucleon and deuteron induced spallation reactions*, Nuclear Physics A 625 (1997) 729-757

[24] Borne F. et al. *Spallation neutron spectra measurements Part I: Time-of-flight technique*, Nuclear Instruments and Methods in Physics Research A 385 (1997) 339-344

[25] Martinez E. et al. *Spallation neutron spectra measurements Part II: Proton recoil spectrometer*, Nuclear Instruments and Methods in Physics Research A 385 (1997) 345-353

[26] Ridikas D., Mittig W. *Neutron production and energy generation by energetic projectiles: protons or deuterons?*, Nuclear Instruments and Methods in Physics Research A 418 (1998) 449-457

[27] Tolstov K. D. *Aspects of Accelerator Breeding*, JINR Dubna preprint 18-89-778 (in Russian)

[28] Hilscher D. et al. *Neutron production by hadron-induced spallation reactions in thin and thick Pb and U targets from 1 to 5 GeV*, Nuclear Instruments and Methods in Physics Research A 414 (1998) 100-116

[29] Dementyev A. V., Sobolevsky N. M., Stavissky Yu. Ya. *Neutron yield from extended lead target under incident protons of 0.1 to 100 GeV*, Nuclear Instruments and Methods in Physics Research A 374 (1996) 70-72

[30] Wagner V. et al. *Neutron Production in Spallation Reactions*, Report UJF-EXP-96/03 of NPI AS CR PRI in Řež (1996) (in Czech)

[31] Firestone R. B. *Table of Isotopes*, 8th Edition, John Wiley & Sons, New York, 1998

[32] Letourneau A. et al. *Neutron production in bombardments of thin and thick W, Hg, Pb targets by 0.4, 0.8, 1.2, 1.8 and 2.5 GeV protons*,

Nuclear Instruments and Methods in Physics Research B 170 (2000) 299-322

[33] Lott B. et al. *Neutron multiplicity distributions for 200 MeV proton, deuteron, and ^{4}He-induced spallation reactions in thick Pb targets*, Nuclear Instruments and Methods in Physics Research A 414 (1998) 117-124

[34] Barashenkov V. S., Nucl. Part. Phys. 9 (1978) 781

[35] Vasilkov R. G., Yurevich V. I., Proc. 11th Meeting of Int. Collaboration on Advanced Neutron Sources ICANS- 11 KEK, Tsukuba, Japan, October 22-26, 1990, KEK Report 90-25 vol. 1 (1991) 340

[36] Akopyan A. G., Kolmichkov N. V., Kuzin A. V., Atomn. Energ. 75 (1993) 219

[37] *Experimental Nuclear Reaction Data (EXFOR/CSISRS)* [http://www.nndc.bnl.gov/exfor]

[38] Chadwick M. B. et al. *ENDF/B-VII.0: Next Generation Evaluated Nuclear Data Library for Nuclear Science and Technology*, Nuclear Data Sheets 107 (2006) 2931-3060 [http://www.nndc.bnl.gov/exfor/endf00.htm]

[39] Heilbron J. L., Seidel R. W., Wheaton B. R. *Lawrence and His Laboratory: A Historian's View of the Lawrence Years*, 1996 Web Publication [http://www.lbl.gov/Science-Articles/Research-Review/Magazine/1981/]

[40] Vasilkov R. G. et al., *Neutron Multiplication in Uranium Bombarded by 300-660 MeV Protons*, Atomnaya Energiya 48 (1978) 329-335 (in Russian)

[41] Voronko V. A. et al. *Energy spectra of neutrons generated by relativistic nuclei in extended lead target*, Atomic Energy 71 (1991) 1028-1030

[42] Mukaiyama T. *Omega programme in Japan and ADS development at JAERI*, Proceedings of an Advisory Group meeting held in Taejon, Republic of Korea, 1-4 November 1999

[43] Carminati F. et al. *An energy amplifier for cleaner and inexhaustible nuclear energy production driven by a particle beam accelerator*, CERN report CERN/AT/93-47(ET)

[44] Rubbia C. et al. *Conceptual design of a fast neutron operated high power energy amplifier*, CERN report CERN/AT/95-44 (ET)

[45] Degweker S. B. et al. *The Physics of Accelerator Driven Sub-critical Reactors*, Workshop on physics of accelerator driven sub-critical system for energy and transmutation, University of Rajasthan, India, January 23-25, 2006

[46] Lawrence G. *Transmutation and Energy Production with Power Accelerators* [http://accelconf.web.cern.ch/AccelConf/p95/Articles/fpd/fpd03.pdf]

[47] Bowman C. D. and Thorson I. M. *Transmutation of Commercial Waste Should Precede Geological Storage*, Radiation Protection Dosimetry 95 (2001) 267-272

[48] Abbondanno U. et al. *CERN n_TOF Facility: Performance Report*, CERN/INTC-O-011, Geneva, 31 January 2003

[49] Borcea C. et al. *Results from the commissioning of the n_TOF spallation neutron source at CERN*, Nuclear Instruments and Methods in Physics Research A 513 (2003) 524-537

[50] Andriamonje S. et al. *Experimental determination of the energy generated in nuclear cascades by a high energy beam*, Physics Letters B 348 (1995) 697-709

[51] Abánades A. et al. *Results from the TARC experiment: spallation neutron phenomenology in lead and neutron-driven nuclear transmutation by adiabatic resonance crossing*, Nuclear Instruments and Methods in Physics Research A 478 (2002) 577-730

[52] Wagner W. et al. *MEGAPIE at SINQ – The first liquid metal target driven by a megawatt class proton beam*, Journal of Nuclear Materials 377 (2008) 12-16

[53] Leray S. et al. *Spallation neutron production by 0.8, 1.2, and 1.6 GeV protons on various targets*, Phys. Rev. C 65 (2002) 044621

[54] Billebaud A. et al. *Prompt multiplication factor measurements in subcritical systems: From MUSE experiment to a demonstration ADS*, Progress in Nuclear Energy 49 (2007) 142-160

[55] Rubbia C. *The TRADE Experiment: state of the project and physics of the spallation target*, PHYSOR 2004 Topical Meeting, Chicago, USA, April 25-29 2004

[56] Ciavola G. *The TRASCO High Power Proton Source and its LEBT*, Proceedings of the 2002 LINAC Conference Gyeongju (Rep. of Korea) 18-22 August 2002

[57] Aït Abderrahim H. *MYRRHA: A multipurpose accelerator driven system for research & development*, Nuclear Instruments and Methods in Physics Research A 463 (2001) 487-494

[58] *Independent Evaluation of the MYRRHA Project*, Report by an International Team of Experts, NEA No. 06881 (2009), ISBN: 978-92-64-99114-9

[59] Gentil E. Le et al. *Exclusive measurements on $^{56}Fe+p$ at 1 A Gev with the SPALADIN setup at GSI*, Nuclear Instruments and Methods in Physics Research A 562 (2006) 743-6

[60] Persson C-M. et al. *Analysis of reactivity determination methods in the subcritical experiment Yalina*, Nuclear Instruments and Methods in Physics Research A 554 (2005) 374-383

[61] Leray S. *HINDAS High-Energy Programme: Main conclusions and implications for spallation neutron sources*, Proceedings of the International Workshop on Nuclear Data for the Transmutation of Nuclear Waste. GSI-Darmstadt, Germany, September 1-5, 2003, ISBN 3-00-012276-1

[62] Westmeier W. et al. *Transmutation experiments on ^{129}I, ^{139}La and ^{237}Np using the Nuclotron accelerator*, Radiochimica Acta 93 (2005) 65

[63] Wan J. S. et al. *Transmutation of ^{129}I and ^{237}Np using spallation neutrons produced by 1.5, 3.7 and 7.4 GeV protons*, Nuclear Instruments and Methods in Physics Research A 463 (2001) 634-652

[64] Adam J. et al. *Investigation of cross-sections for the formation of residual nuclei in reactions induced by 660 MeV protons interacting with natural uranium targets*, Proceedings of the International Workshop on Nuclear Data for the Transmutation of Nuclear Waste, GSI-Darmstadt, Germany, September 1-5, 2003, ISBN 3-00-012276-1

[65] Adam J. et al. *Investigation of formation of residual nuclei in reactions induced by 660 MeV protons interacting with the radioactive* ^{237}Np, ^{239}Pu, ^{129}I, Proceedings of the International Conference on Nuclear Data for Science and Technology - ND 2001, Tsukuba, October 7-12, 2001. Journal of Nuclear Science and Technology (2002) 272-5

[66] Pronskikh V. S. et al. *Study of 660 MeV proton-induced reactions on* ^{129}I, Intern. Conf. on Nuclear Data for Science and Technology ND 2004, Santa Fe, New Mexico, 26 September - 1 October 2004, AIP conference proceedings 769 (2005) 1047-50

[67] Gustov S. A. et al. *Design Status and Future Research Programme for a Sub-critical Assembly Driven by a Proton Accelerator with Proton Energy 660 MeV for Experiments on Long-lived Fission Products and Minor Actinides Transmutation (SAD)*, 7th Information Exchange Meeting on Actinide and Fission Product Partitioning and Transmutation, 14-16 October 2002, Jeju, Republic of Korea

[68] Shvetsov V. et al. *The Subcritical Assembly in Dubna (SAD)-Part I: Coupling all major components of an Accelerator Driven System (ADS)*, Nuclear Instruments and Methods in Physics Research A 562 (2006) 883-886

Gudowski W. et al. *The Subcritical Assembly in Dubna (SAD)-Part II: Research program for ADS-demo experiment*, Nuclear Instruments and Methods in Physics Research A 562 (2006) 887-891

Barashenkov V. S., *Targets for Accelerator-Driven System SAD*, Pisma v Zhurnal Fizika Elementarnykh Chastits i Atomnogo Yadra 131 (2006) 101-104 (in Russian); Physics of Particles and Nuclei Letters 3 (2006) 131-133

[69] Krivopustov M. I. et al. *First experiments on transmutation studies of* ^{129}I *and* ^{237}Np *using relativistic protons of 3.7 GeV*, Journal of Radioanalytical and Nuclear Chemistry 222 (1997) 267-270; JINR Dubna preprint E1-97-59

[70] Krivopustov M. I. et al. *First experiments with a large uranium blanket within the installation "energy plus transmutation" exposed to 1.5 GeV protons*, Kerntechnik 68 (2003) 48-54

[71] Krivopustov M. I. et al. *Investigation of Neutron Spectra and Transmutation of* ^{129}I, ^{237}Np *and Other Nuclides with 1.5 GeV Protons from*

the Dubna Nuclotron Using the Electronuclear Installation "Energy plus Transmutation", JINR Dubna preprint E1-2004-79

[72] Katovský K. et al. *Transmutation of ^{238}Pu and ^{239}Pu using neutrons produced in target-blanket system "Energy plus Transmutation" bombarded by relativistic protons*, Proceedings of the IYNC2004 conference, Canadian Nuclear Society, 2005

[73] Zhuk I. V. et al. *Investigation of energy-space distribution of neutrons in the lead target and uranium blanket within the installation "Energy plus Transmutation" exposed to 1.5 GeV protons*, JINR Dubna preprint P1-2002-184 (in Russian)

[74] Zhuk I. V. et al. *Determination of spatial and energy distributions of neutrons in experiments on transmutation of radioactive waste using relativistic protons*, Radiation Measurements 31 (1999) 515-520

[75] Zamani M. et al. *Neutron yields from massive lead and uranium targets irradiated with relativistic protons*, Radiation Measurements 40 (2005) 410-414

[76] Chultem D. et al. *Investigation of fast neutron spectra of the installation "Energy plus Transmutation" at the 1.5 GeV proton beam of the Nuclotron*, JINR Dubna preprint P1-2003-59 (in Russian)

[77] Manolopoulou M. et al. *Studies on the response of 3He and 4He proportional counters to monoenergetic fast neutrons*, Nuclear Instruments and Methods in Physics Research A 562 (2006) 371-9

[78] Wagner V., Kugler A., Filip C., Kovář P. *Experimental Study of Neutron Production in Proton Reactions with Heavy Targets*, Proceedings of Experimental Nuclear Physics in Europe Facing the Next Millennium Conference - ENPE99, Seville, Spain, June 21-26 1999

[79] Kugler A., Wagner V., Filip C. *Experimental Study of Neutron Fields Produced in Proton Reactions with Heavy Targets*, Proceedings of the 3^{rd} International Conference on Accelerator Driven Transmutation Technologies and Applications - ADTTA'99, Prague (Průhonice), 7 - 11 June, 1999

[80] Henzl V. et al. *Transmutation of ^{129}I with High Energy Neutrons Produced in Spallation Reactions Induced by Protons in Massive Target*,

Proceedings of the International Conference on Nuclear Data for Science and Technology - ND 2001, Tsukuba, October 7-12, 2001. Journal of Nuclear Science and Technology 2 (2002) 1248-51

[81] Henzl V. et al. *Experimental study of high energy neutrons produced in spallation reactions induced by protons in massive target and transmutation of* ^{129}I, Contributions of the AccApp/ADTTA'01 meeting in Reno, November 2001

[82] Henzl V. et al. *Study of* ^{129}I *Transmutation by High Energy Neutrons Produced in Lead Spallation Target*, Proceedings of the International Workshop on Nuclear Data for the Transmutation of Nuclear Waste, GSI-Darmstadt, Germany, September 1-5, 2003, ISBN 3-00-012276-1

[83] Krása A. et al. *Experimental Studies of Spatial Distributions of Neutron Production Around Thick Lead Target Irradiated by 0.9 GeV Protons*, Proceedings of the International Workshop on Nuclear Data for the Transmutation of Nuclear Waste, GSI-Darmstadt, Germany, September 1-5, 2003, ISBN 3-00-012276-1

[84] Krása A. et al. *Neutron Production in Spallation Reactions of 0.9- and 1.5-GeV Protons on a Thick Lead Target - Comparison of Experimental Data and MCNPX Simulations*, International Conference on Nuclear Data for Science and Technology 2004, Santa Fe, New Mexico, 26th September-1st October 2004. AIP Conference Proceedings, Volume 769 (2005) 1555-9

[85] Majerle M. et al. *Experimental Studies of Transmutation of* ^{129}I *by Spallation Neutrons using JINR Dubna Phasotron*, in Proceedings of the XVII International Baldin Seminar on High Energies Physics Problem, Dubna, Russia, September 27 - October 2, 2004. Relativistic Nuclear Physics and Quantum Chromodynamics vol. II (2005) 135-140

[86] Wagner V. et al. *Experimental Studies of Spatial Distributions of Neutrons Produced by Set-ups with Thick Lead Target Irradiated by Relativistic Protons*, in Proceedings of the XVII International Baldin Seminar on High Energies Physics Problem, Dubna, Russia, September 27 - October 2, 2004. Relativistic Nuclear Physics and Quantum Chromodynamics vol. II (2005) 111-116

[87] Krása A. et al. *Neutron Production in Spallation Reactions of 0.9 and 1.5 GeV Protons on a Thick Lead Target Comparison between Experimental Data and Monte-Carlo Simulations*, JINR Dubna Preprint E1-2005-46

[88] Majerle M. et al. *MCNPX benchmark tests of neutron production in massive lead target*, Proceedings from International Topical Meeting on Mathematics and Computation, Supercomputing, Reactor Physics and Nuclear and Biological Applications - M&C 2005, Palais des Papes, Avignon, France, September 12-15, 2005, on CD-ROM, American Nuclear Society, LaGrange Park, IL (2005)

[89] Majerle M. et al. *Experimental studies and simulations of spallation neutron production on a thick lead target*, NPDC 19 – New Trends in Nuclear Physics Applications and Technology. Pavia (Italy) September 5-9, 2005; Journal of Physics: Conference Series 41 (2006) 331-339

[90] Krása A. et al. *Comparison between experimental data and Monte-Carlo simulations of neutron production in spallation reactions of 0.7-1.5 GeV protons on a thick, lead target*, NPDC 19 – New Trends in Nuclear Physics Applications and Technology. Pavia (Italy) September 5-9, 2005; Journal of Physics: Conference Series 41 (2006) 306-314

[91] Wagner V. et al. *The Possibility to Use "Energy plus Transmutation" Setup for Neutron Production and Transport Benchmark Studies*, Workshop on physics of accelerator driven sub-critical system for energy and transmutation, University of Rajasthan, India, 23-25 January 2006; PRAMANA - Journal of Physics 68 (2007) 297-306

[92] Křížek F. et al. *The study of spallation reactions, neutron production and transport in a thick lead target and a uranium blanket during 1.5 GeV proton irradiation*, Czechoslovak Journal of Physics 56 (2006) 243-252

[93] Svoboda O. et al. *Neutron Production in Pb/U Assembly Irradiated by Protons and Deuterons at 0.7–2.52 GeV*, in Proceedings of the International Conference on Nuclear Data for Science and Technology ND2007, Nice, France, 23-27 April 2007, pp. 1197-1200

[94] Majerle M. et al. *MCNPX simulations of the experiments with relativistic protons directed to thick, lead targets*, Nuclear Instruments and Methods in Physics Research A 580 (2007) 110-3

[95] Krása A. et al. *Neutron Emission in the Spallation Reactions of 1 GeV Protons on a Thick, Lead Target Surrounded by a Uranium Blanket*, JINR Dubna Preprint E15-2007-81

[96] Majerle M. et al. *Monte Carlo studies of the Energy plus Transmutation system*, JINR Dubna Preprint E15-2007-82

[97] Jungclas H. et al. *A mobile helium-jet transport system for on-line spectroscopy of short-range spallation products*, Nuclear Instruments and Methods 137 (1976) 93-8

[98] Prael R. E., Lichtenstein H. *User Guide to LCS: The LAHET Code System*, LANL report LA-UR-89-3014 (1989)

[99] Briesmeister J. F., Editor. *MCNP – A General Monte Carlo N-Particle Transport Code Version 4B*, LANL report LA-12625-M (1997)

[100] Pelowitz D. B. et al. *MCNPX Users's manual. Version 2.5.0*, LANL report LA-CP-05-0369 (2005)

[101] Hendricks J. S. et al. *MCNPX, VERSION 2.6.C*, LANL report LA-UR-06-7991 (2006)

[102] Ferrari A. et al. *FLUKA: a multi-particle transport code (program version 2005)*, CERN 2005-10 (2005), INFN/ TC_05/11, SLAC-R-773

[103] Radiation Shielding Information Center *HETC Monte Carlo High-Energy Nucleon-Meson Transport Code*, ORNL Report CCC-178 (1977)

[104] Coleman W. A., Armstrong T. W. *The Nucleon-Meson Transport Code NMTC*, ORNL Report 4606 (1970)

[105] Cugnon J., Volant C., Vuillier S. *Improved intranuclear cascade model for nucleon-nucleus interactions*, Nuclear Physics A 620 (1997) 475-509

[106] Dementyev A. V., Sobolevsky N. M. *SHIELD – universal Monte Carlo hadron transport code: scope and applications*, Radiation Measurements 30 (1999) 553-557

[107] Barashenkov V. S. *Monte Carlo simulation of ionization and nuclear processes initiated by hadron and ion beams in media*, Computer Physics Communications 126 (2000) 28-31

Barashenkov V. S., *CASCADE/INPE code system*, Atomnaya Energiya 87 (1999) 283-286 (in Russian); Atomic Energy 87 (1999) 742-4

[108] Gudima K. K., Mashnik S. G., Toneev V. D. *Cascade-exciton model of nuclear reactions*, Nuclear Physics A 401 (1983) 329-361

[109] Gudima K. K., Mashnik S. G., Sierk A. J. *User manual for the code LAQGSM*, LANL Report LA-UR-01-6804 (2001)

[110] Furihata S. *Statistical analysis of light fragment production from medium energy proton-induced reactions*, Nuclear Instruments and Methods in Physics Research B 171 (2000) 251-8

[111] Agostinelli S. et al. *GEANT4 – a simulation toolkit*, Nuclear Instruments and Methods in Physics Research A 506 (2003) 250-303

[112] Niita K. et al. *High-energy particle transport code NMTC/JAM*, Nuclear Instruments and Methods in Physics Research B 184 (2001) 406-420

[113] Azhgirey I. L. et al. *The future development of the MARS program for the electromagnetic cascades simulation in the energy range up to 20 TeV*, IHEP Protvino preprint 93-19 (in Russian)

Azhgirey I. L., Talanov V. V., *MARS program package status*, in: Materials of the 17th Workshop on the Charged Particles Accelerators (RUPAC-2000), vol. 2, Protvino, Russia (2000) 184-7 (in Russian)

[114] Bersillon O. et al. *TIERCE: A code System for particles and Radiation Transport in Thick targets*, in Proceedings of Second Conference on Accelerator-Driven Transmutation Technologies and Applications, 3−7 June 1996, Kalmar, Sweden (1997) 520-6

[115] Duarte H. *Particle production in nucleon induced reactions above 14 MeV with an intranuclear cascade model*, Physical Review C 75 (2007) 024611

Duarte H. *The nonelastic reaction code BRIEFF and its intranuclear cascade BRIC*, in Proceedings of the International Conference on Nuclear Data for Science and Technology ND2007, Nice, France, 23-27 April 2007

[116] Bielajew A. F. *Fundamentals of the Monte Carlo method for neutral and charged particle transport*, University of Michigan, 2001 [http://www-personal.umich.edu/ bielajew/MCBook/book.pdf]

[117] Waters L. S. et al. *MCNPX Users's manual. Version 2.1.5*, LANL report LA-UR-99-1995 (1999)

[118] Bertini H. W. *Low-Energy Intranuclear Cascade Calculation*, Physical Review 131 (1963) 1801

[119] Yariv Y., Fraenkel Z. *Intranuclear cascade calculation of high energy heavy ion collisions: Effect of interactions between cascade particles*, Phys. Rev. C 24 (1981) 488-494

[120] Boudard A. et al. *Intranuclear cascade model for a comprehensive description of spallation reaction data*, Phys. Rev. C 66 (2002) 044615

[121] Pienkowski L. et al. *Hot nuclei in reactions induced by 475 MeV, 2 GeV* ^{1}H *and 2 GeV* ^{3}He, Physics Letters B 336 (1994) 147-151

[122] Trebukhovsky Yu. V. et al. *Double-Differential Cross Sections for the Production of Neutrons from Pb, W, Zr, Cu, and Al Targets Irradiated with 0.8-, 1.0-, and 1.6-GeV Protons*, Yadernaya Fizika 68 (2005) $4-16$ (in Russian); Physics of Atomic Nuclei 68 (2005) $3-15$

[123] Prael R. E., Bozoian M. *Adaptation of the Multistage Pre-equilibrium Model for the Monte Carlo Method (I)*, LANL Report LA-UR-88-3238 (1998)

[124] Gudima K. K., Ososkov G. A., Toneev V. D. *Model for Pre-Equilibrium Decay of Excited Nuclei*, Yad. Fiz. 21 (1975) 260 (in Russian); Sov. J. Nucl. Phys. 21 (1975) 138

Mashnik S. G., Toneev V. D. *MODEX – the Program for Calculation of the Energy Spectra of Particles Emitted in the Reactions of Pre-Equilibrium and Equilibrium Statistical Decays*, JINR Dubna preprint P4-8417 (1974)

[125] Dresner L. *EVAP-A Fortran Program for Calculating the Evaporation of Various Particles from Excited Compound Nuclei*, ORNL Report ORNL-TM-196 (1962)

[126] Junghans A. R. et al. *Projectile-fragment yields as a probe for the collective enhancement in the nuclear level density*, Nuclear Physics A 629 (1998) 635-655

[127] Barish J. et al. *HETFIS High-Energy Nucleon-Meson Transport Code with Fission*, ORNL Report ORNL-TM-7882 (1981)

[128] Atchison F. *Spallation and Fission in Heavy Metal Nuclei under Medium Energy Proton Bombardment*, Meeting on Targets for Neutron Beam Spallation Sources, Kernforschungsanlage Jülich GmbH (1980) 17-46

[129] Chadwick M. B. et al. *Cross-Section Evaluations to 150 MeV for Accelerator-Driven Systems and Implementation in MCNPX*, Nuclear Science and Engineering 131 (1999) 293-328

[130] Koning A. J. et al. *New Nuclear Data Evaluations for Ca, Sc, Fe, Ge, Pb, and Bi Isotopes*, International Conference on Nuclear Data for Science and Technology 2004, Santa Fe, New Mexico, 26th September-1st October 2004. AIP Conference Proceedings, Volume 769 (2005) 422-5

[131] *An Introduction to the ENDF Formats*, LANL report LA-UR-98-1779 (1998) [http://t2.lanl.gov/endf/title.html]

[132] Chadwick M. B. et al. *Physics models and nuclear data evaluations for enhanced Monte-Carlo transport*, LANL report LA-UR-00-3601 (2000)

[133] Fukahori T. *Historical overview of nuclear data evaluation in the intermediate energy region*, International Conference on Nuclear Data for Science and Technology 2004, Santa Fe, New Mexico, 26th September-1st October 2004. AIP Conference Proceedings, Volume 769 (2005) 47-52

[134] Leray S. et al. *Validation of high-energy nuclear models: State-of-the-art and perspectives*, Nuclear Instruments and Methods in Physics Research A 562 (2006) 806-9

[135] van der Meer K. et al. *Spallation yields of neutrons produced in thick lead/bismuth targets by protons at incident energies of 420 and 590 MeV*, Nuclear Instruments and Methods in Physics Research B 217 (2004) 202-220

[136] Ishibashi K. et al. *Measurement of neutron-production double-differential cross sections for nuclear spallation reaction induced by 0.8, 1.5 and 3.0 GeV protons*, Journal of Nuclear Science and Technology 34 (1997) 529-537

[137] Meigo S. et al. *Measurements of neutron spectra produced from a thick lead target bombarded with 0.5- and 1.5-GeV protons*, Nuclear Instruments and Methods in Physics Research A 431 (1999) 521-530

[138] Meigo S. et al. *Measurements of Neutron Spectra Produced from a Thick Tungsten Target Bombarded with 1.1 and 2.3 GeV/c Protons and π^+ Mesons*, 1999 Symposium on Nuclear Data (JAERI-Conf 2000-005), Nov. 18-19, 1999 at Tokai Establishment of JAERI

[139] Takada H. *Nuclear medium effects in the intranuclear cascade calculation*, Journal of Nuclear Science and Technology 33 (1996) 275-282

[140] Yoshizawa N. et al. *Development of high energy transport code HETC-3STEP applicable to the nuclear reaction with incident energies above 20 MeV*, Journal of Nuclear Science and Technology 32 (1995) 601-7

[141] Koning A. J., Hilaire S., Duijvestijn M. C. *TALYS: Comprehensive Nuclear Reaction Modeling*, International Conference on Nuclear Data for Science and Technology 2004, Santa Fe, New Mexico, 26th September-1st October 2004. AIP Conference Proceedings, Volume 769 (2005) 1154-9

[142] Koning A. J., Hilaire S., Duijvestijn M. C. *TALYS-1.0 A nuclear reaction program*, User manual, December 21, 2007

[143] Broeders C. H. M., Konobeyev A. Yu., Mercatali L. *Global Comparison of TALYS and ALICE Code Calculations and Evaluated Data from ENDF/B, JENDL, FENDL, and JEFF Files with Measured Neutron Induced Reaction Cross-sections at Energies above 0.1 MeV*, Journal of Nuclear and Radiochemical Sciences 7 (2006) pp. N1-N4

[144] Young P. G., Arthur E. D., Chadwick M. B. *Comprehensive nuclear model calculations: theory and use of the GNASH code*, in Proceedings of the IAEA Workshop on Nuclear Reaction Data and Nuclear Reactors, ICTP Trieste, Italy, April 15-May 17, 1996 (World Sci. Publ. Co., Singapore, 1998) 227-404

[145] Broeders C. H. M. et al. *ALICE/ASH - Pre-compound and evaporation model code system for calculation of excitation functions, energy and angular distributions of emitted particles in nuclear reactions at intermediate energies*, Report Forschungszentrum Karlsruhe FZKA 7183 (2006)

[146] Uhl M., Strohmaier B. *Computer code for particle induced activation cross sections and related quantities*, IRK report No. 76/01, Vienna (1976)

[147] Herman M. et all. *EMPIRE: Nuclear Reaction Model Code System for Data Evaluation*, Nuclear Data Sheets 108 (2007) 2655-2715